

Supplemental Data

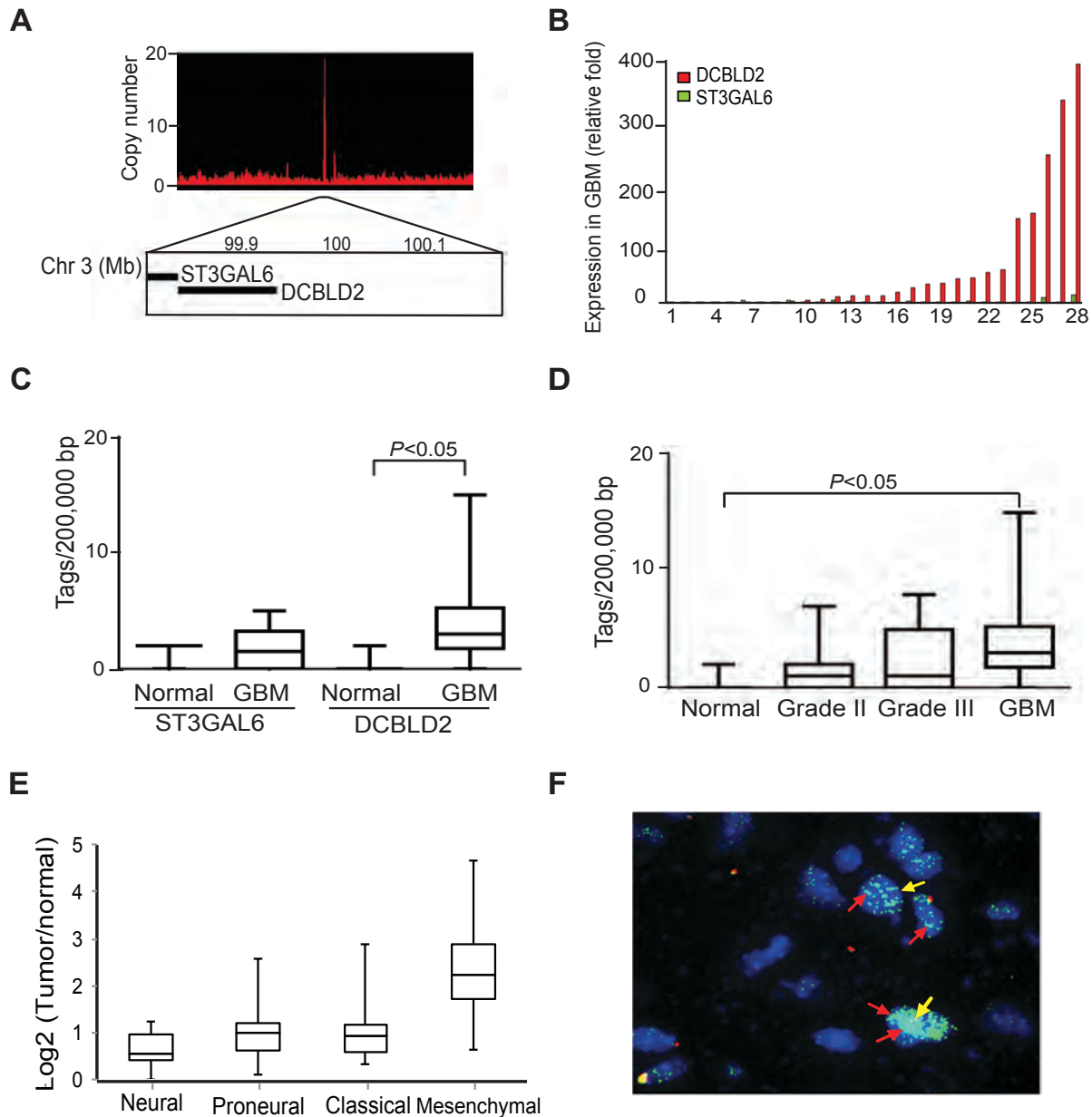
Journal: **Journal of Clinical Investigation**

EGFR Phosphorylation of DCBLD2 Recruits TRAF6 and Stimulates

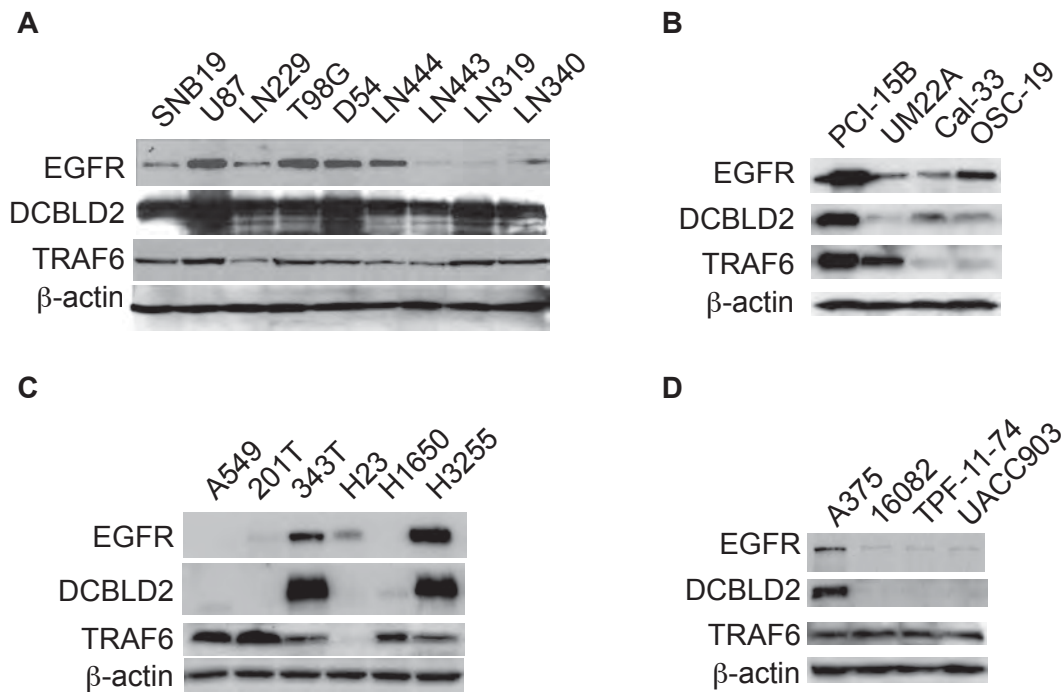
Akt-promoted Tumorigenesis

Haizhong Feng, Giselle Y. Lopez, Chung Kwon Kim, Angel Alvarez, Christopher G. Duncan, Ryo Nishikawa, Motoo Nagane, An-Jey Su, Philip E. Auron, Matthew L. Hedberg, Lin Wang, Jeffery J. Raizer, John A. Kessler, Andrew T. Parsa, Wei-Qiang Gao, Sung-Hak Kim, Mutsuko Minata, Ichiro Nakano, Jennifer R. Grandis, Roger E. McLendon, Darell D. Bigner, Hui-Kuan Lin, Frank B. Furnari, Webster K. Cavenee, Bo Hu, Hai Yan and Shi-Yuan Cheng

Supplemental Figures 1-24 and Supplemental Tables 1-2



Supplementary Figure 1. Genomic expression of *DCBLD2* gene is up-regulated in clinical GBMs. (A) Digital karyotyping reveals a focal region on chromosome 3q12.1 displaying high copy numbers that indicate gene amplification. This amplified region includes two genes, *ST3GAL6* and *DCBLD2*. (B) Quantitative real time reverse transcription PCR (Q-PCR) identifies increased expression of *DCBLD2* but not *ST3GAL6* in 14 out of 28 clinical GBM tumors. (C) Serial analysis of gene expression (SAGE) of *DCBLD2* and *ST3GAL6* in GBMs. Box, 25th-75th percentile with median. Whiskers, minimum and maximum values. (D) SAGE of *DCBLD2* in subsets of gliomas. Normal vs. GBM, $P < 0.05$. Box, 25th-75th percentile with median. Whiskers, minimum and maximum values. (E) Genomic expression of *DCBLD2* among GBM subtypes ($n = 116$). Number of GBM tumors, neural, 19, proneural, 37, classical, 22 and mesenchymal, 38. $P < 0.001$ for mesenchymal vs. neural, mesenchymal vs. proneural, mesenchymal vs. classical. (F) Interphase FISH in a clinical GBM tumor TB2580 identifies tumor cells with amplification of *DCBLD2* (green, FITC) compared to a chromosome 3 reference control (red, TRITC). Nuclei are stained blue (DAPI). Red arrows, *DCBLD2* probe. Yellow arrows, Chromosome 3 reference probe. Overlap of *DCBLD2* and chromosome 3 probes produces white-dish color indicated by yellow arrows. Data are derived from The Cancer Genome Anatomy Project (C and D) or The Cancer Genome Atlas (TCGA, E).



Supplementary Figure 2. Expression of EGFR, DCBLD2, and TRAF6 in cell lines derived from human glioma, lung cancer, HNC and melanoma.

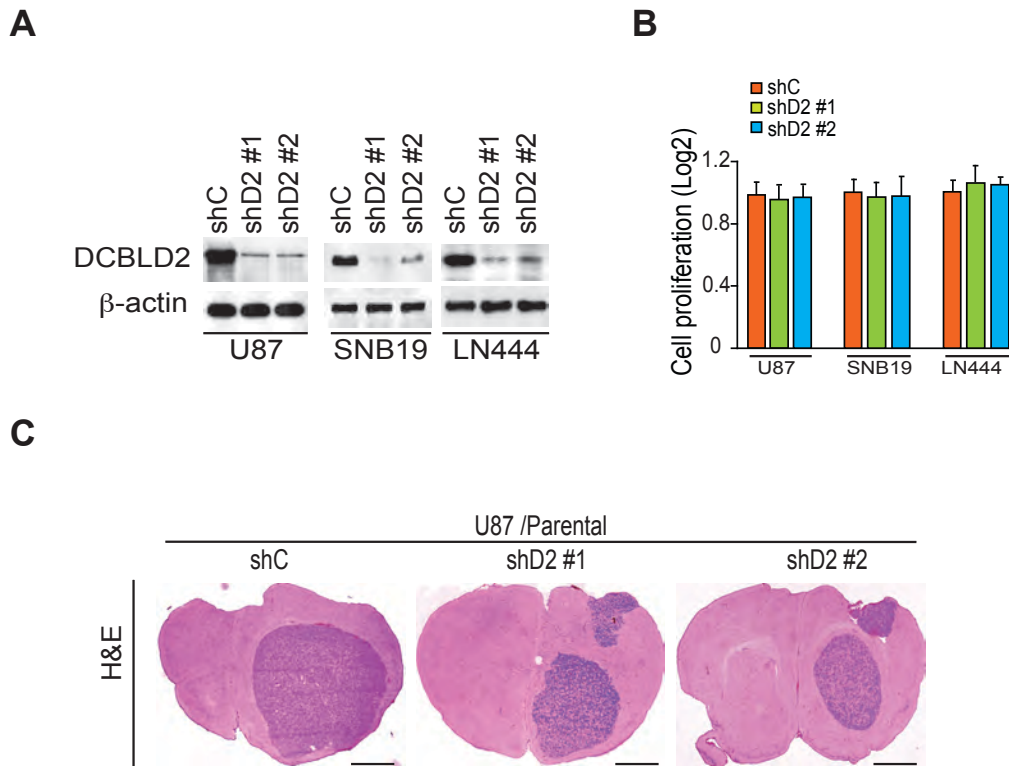
A. Expression of EGFR, DCBLD2 and TRAF6 in nine glioma cell lines.

B. Expression of EGFR, DCBLD2 and TRAF6 in four HNC lines.

C. Expression of EGFR, DCBLD2 and TRAF6 in six lung cancer cell lines.

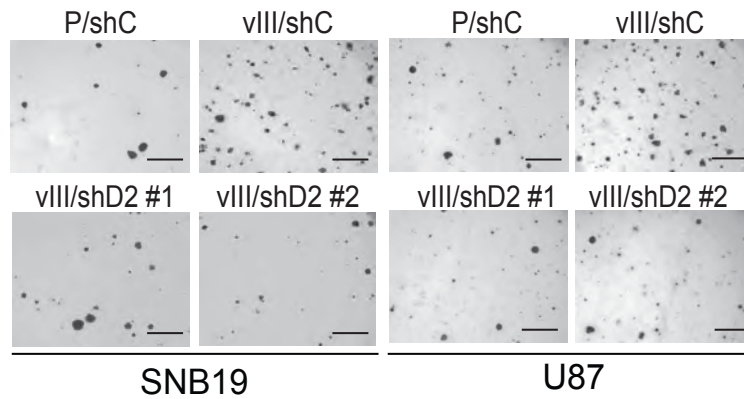
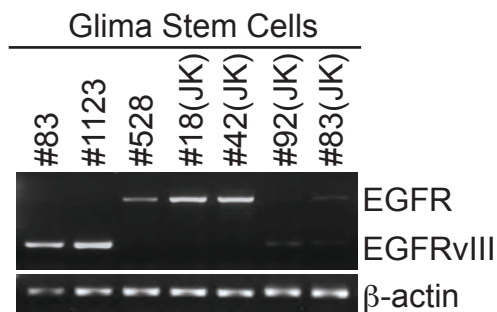
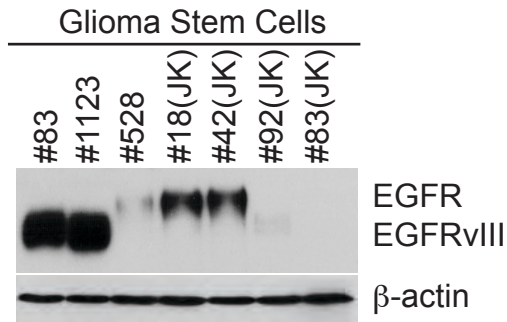
D. Expression of EGFR, DCBLD2 and TRAF6 in four melanoma cell lines.

β-actin was used as a loading control. Data are representative of three independent experiments.



Supplementary Figure 3. Knockdown of endogenous DCBLD2 showed minimal effect on glioma cell proliferation *in vitro* and a modest impact on glioma tumor growth in the brain.

- A.** Knockdown of endogenous DCBLD2 by two different shRNAs (shD2#1, shD2#2) in glioma U87, SNB19 and LN444 cells. IB analysis. β -actin was used as a loading control.
- B.** Depletion of endogenous DCBLD2 did not affect *in vitro* cell proliferation of glioma cells. Cell proliferation of indicated glioma cells was determined by WST-1 assays using serum-starved glioma cells from panel **A**. Cells were seeded in 6 replicates. Error bars, \pm SD.
- C.** Inhibition of DCBLD2 by shRNA knockdown only displayed a modest impact on tumorigenesis of glioma U87 cells in the brain of mice. Representative images of H&E stained brain sections with indicated U87 gliomas from 5 mice per group of two independent experiments. Scale bars, 100 μ m.
Data are representative of two to three independent experiments.

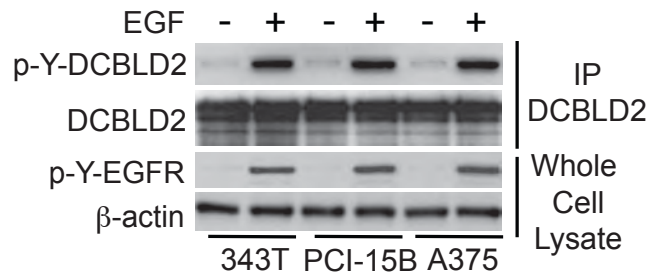
A**B****C**

Supplementary Figure 4. DCBLD2 is required for EGFR-driven glioma tumorigenesis.

(A) Effect of DCBLD2 knockdown by shD2#1, shD2#2 or shC on glioma cell colony formation. Cells were seeded on soft agar in triplicate. Scale bars, 1 mm.

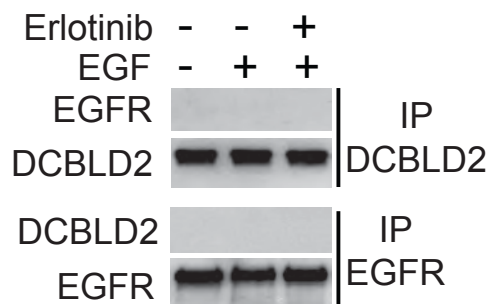
(B) & (C) Analyses of gene expression of WT EGFR or EGFRvIII in various patient-derived glioma stem cells (GSC) by RT-PCR using primers that specifically distinguish gene products of WT or EGFRvIII (1) **(B)** or by IB using an anti-EGFR antibody **(C)**.

WT EGFR were detected in GSC528, JK18, JK42 and JK 83 whereas EGFRvIII is expressed in GSC83, 1123 and JK92 cells. Data are representative of two independent experiments.



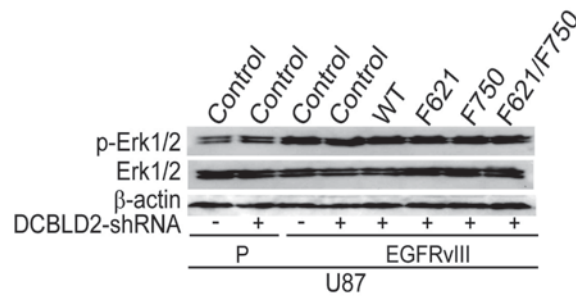
Supplementary Figure 5. EGF stimulates p-Y-DCBLD2 in cell lines derived from lung cancer, HNC and melanoma.

IP-IB assays. EGF stimulates p-Y-DCBLD2 in lung cancer 343T, HNC PCI-15B and melanoma A375 cells. Immunoprecipitated p-Y-DCBLD2 was detected with a pan anti-tyrosine antibody, 4G10. p-Y-EGFR was detected with an anti-p-EGFR^{Y1045} antibody. DCBLD2 and β-actin were used as loading controls. Data are representative of three independent experiments.



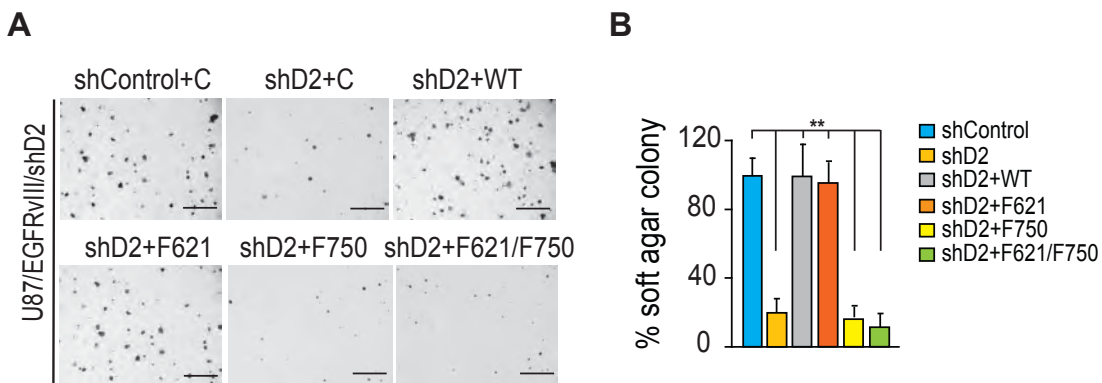
Supplementary Figure 6. Reciprocal IP-IB analyses failed to detect DCBLD2 association to EGFR in glioma cells.

IP-IB assays. Immunoprecipitated DCBLD2 (upper panels) or EGFR (lower panels) was subjected to IB analyses of EGFR and DCBLD2 from U87/EGFR WT cells stimulated with EGF (50 ng/ml, 10 min) with or without pretreatment of EGFR inhibitor, Erlotinib (10 μM, 1h). Data are representative of three independent experiments.



Supplementary Figure 7. Mutant forms of DCBLD2^{F621}, DCBLD2^{F750}, and DCBLD2^{F621/F750} have no effect on EGFRvIII-stimulated Erk1/2 activity.

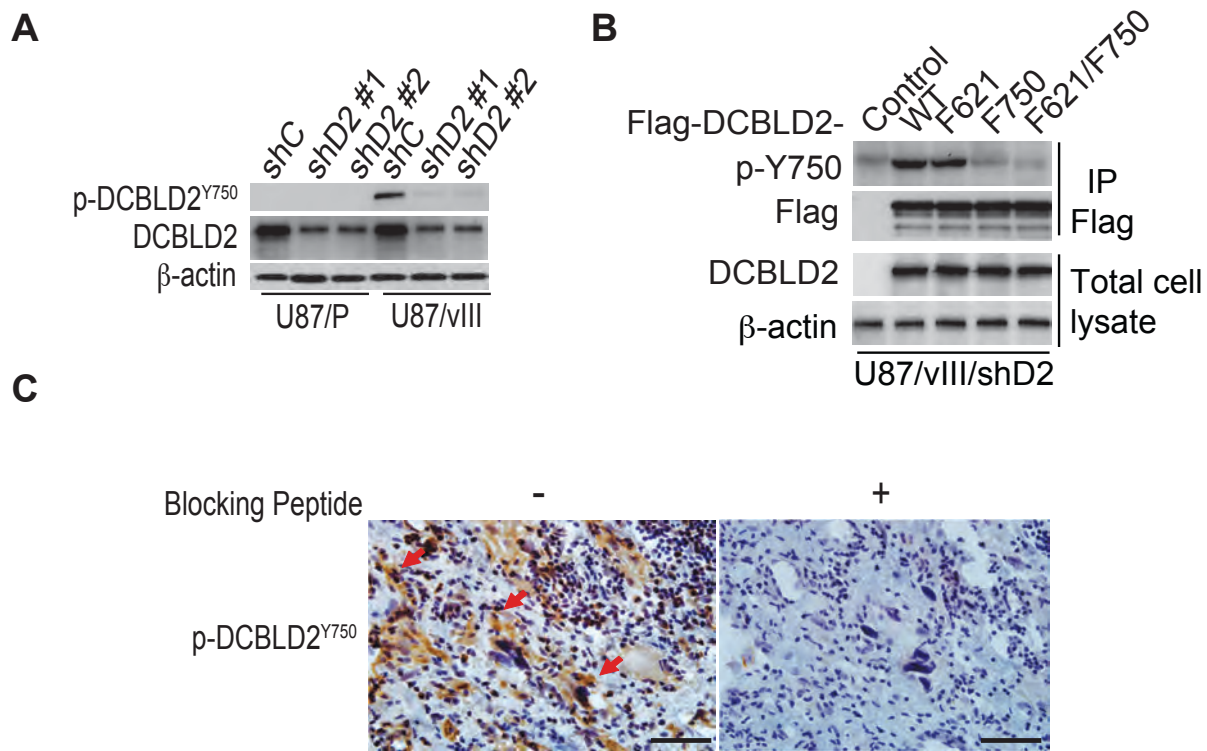
IB analyses of Erk1/2 activity. Re-expression of Flag-DCBLD2 shRNA-resistant DCBLD2^{WT} (WT) or indicated mutants or a vector control does not affect p-Erk1/2 in U87/EGFRvIII/shD2 cells. Erk1/2 and β-actin were used as loading controls. Data are representative of three independent experiments.



Supplementary Figure 8. Re-expression of Flag-DCBLD2 shRNA-resistant DCBLD2^{WT} or DCBLD2^{F621} but not DCBLD2^{F750}, DCBLD2^{F621/F750} mutant, or a vector control (C), rescues EGFRvIII-stimulated soft agar colony formation *in vitro*.

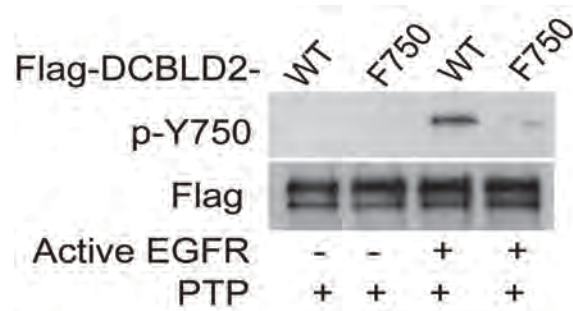
A. Soft agar colony formation assay for U87/EGFRvIII/shD2 that separately re-express shRNA-resistant WT or mutant forms of DCBLD2. Representative images of three independent experiments. Scale bars, 1 mm.

B. Quantifications of soft agar colonies. Error bars from 3 replicates, ± SD. Compared to shControl, **, *P* < 0.01. Data are representative of three independent experiments.



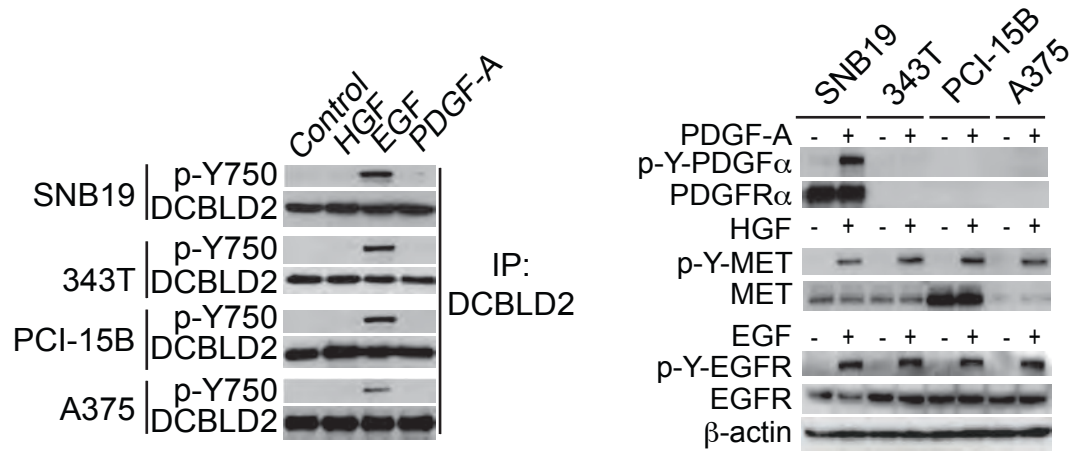
Supplementary Figure 9. Validation of the specificity of the anti-p-DCBLD2^{Y750} antibody.

- A.** IB assays. EGFRvIII activates p-DCBLD2^{Y750} that is inhibited by shRNA knockdown of DCBLD2. The EGFRvIII-stimulated p-DCBLD2^{Y750} was detected with a rabbit anti-p-DCBLD2^{Y750} antibody generated against a specific phospho-peptide containing p-Y750 and surrounding amino acids. β-actin was used as a loading control.
- B.** Re-expression of shRNA-resistant DCBLD2^{WT} and mutant DCBLD2^{F621}, but not DCBLD2^{F750} or DCBLD2^{F621/F750}, rescues the EGFRvIII-stimulated p-DCBLD2^{Y750} in glioma U87/EGFRvIII/shD#2 cells. β-actin was used as a loading control.
- C.** IHC assays of human a clinical GBM tumor tissue with the specific anti-p-DCBLD2^{Y750} antibody in the presence or absence of a specific blocking peptide synthesized with identical amino acid sequence of an immunoreactive peptide for generating this specific anti-p-DCBLD2^{Y750} antibody including the Y750 residue. IHC was performed twice on the GBM sample with the blocking peptide with similar results. Scale bars, 50 μm. Data are representative of two to three independent experiments.



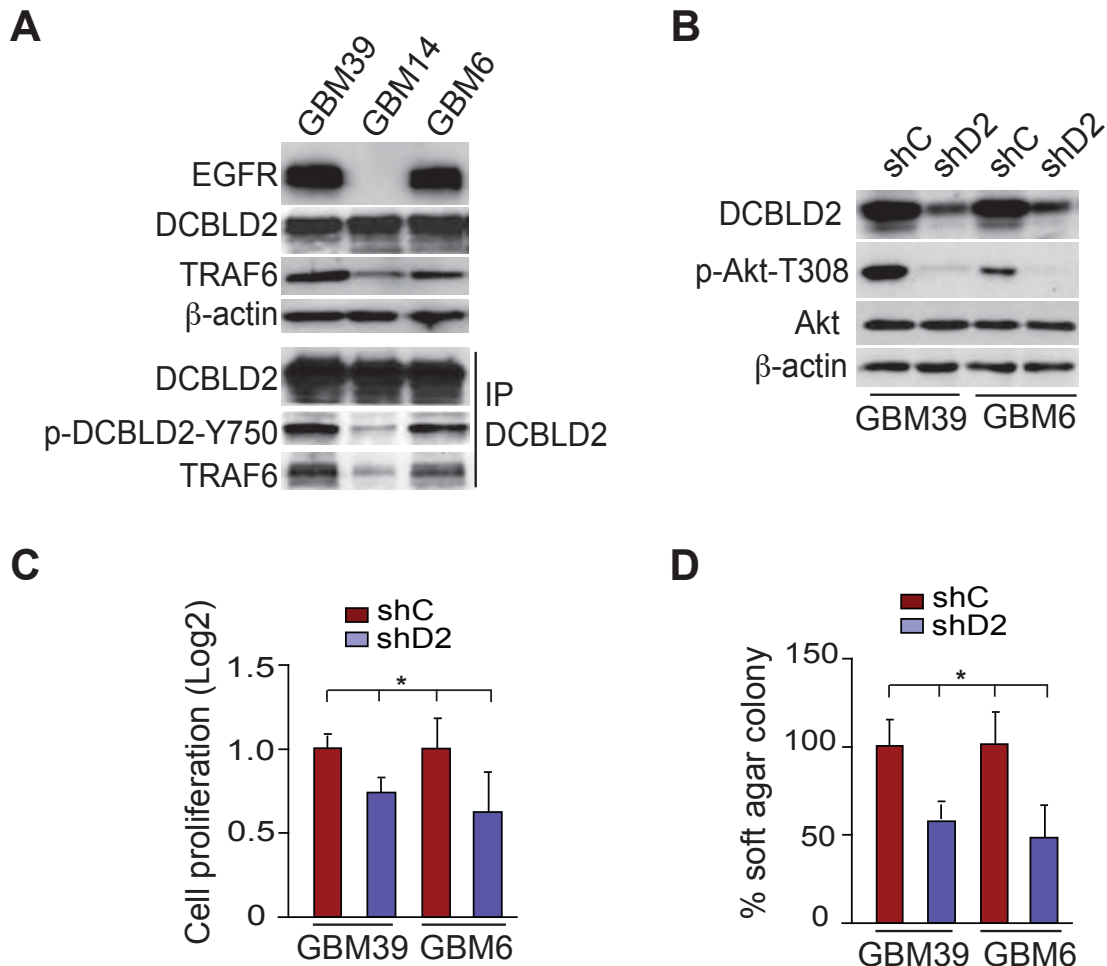
Supplementary Figure 10. EGFR phosphorylates DCBLD2 at Y750 *in vitro*.

In vitro kinase phosphorylation assay. A Flag-tagged DCBLD2^{WT} (WT) or a DCBLD2^{F750} mutant was separately expressed in HEK293T cells and immunoprecipitated with an anti-Flag antibody. The immunoprecipitated DCBLD2 proteins were pre-treated with a recombinant protein tyrosine phosphatase (PTP) and then incubated with or without a recombinant active EGFR. The reaction mixtures were examined by IB analysis using the specific anti-p-DCBLD2^{Y750} antibody. Flag-DCBLD2 was used as a loading control. Data are representative of two independent experiments.



Supplementary Figure 11. p-DCBLD2^{Y750} is stimulated by EGF but not HGF or PDGF-A in various types of human cancer cells.

Glioma SNB19, lung cancer 343T, HNC PCI-15B and melanoma A375 cells were serum-starved for 24 h and treated with or without 50 ng/ml PDGF-A, 100 ng/ml EGF, or 40 ng/ml HGF for 5 min. A specific anti-p-DCBLD2^{Y750} antibody was used to detect p-Y of endogenous DCBLD2 in these cells; anti-c-Met (p-Y1230/Y1234/Y1235), anti-p-PDGFRα (p-Y754) and anti-p-EGFR (p-Y1045) antibodies were used to examine p-Y of c-Met, PDGFRα and EGFR, respectively. DCBLD2, PDGFRα, EGFR, and β-actin were used as loading controls. Data are representative of three independent experiments.



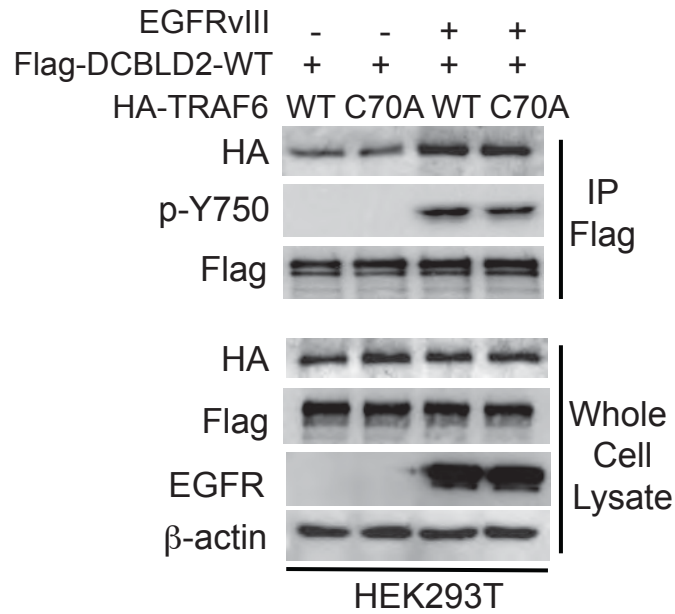
Supplementary Figure 12. Association of DCBLD2 with TRAF6 and effect of knockdown of DCBLD2 on cell proliferation in primary GBM cells with high levels of endogenous EGFRvIII expression.

- A.** IP-IB analyses of association of DCBLD2 with TRAF6. Human primary short-term cultured glioma GBM6 and GBM39 cells express endogenous EGFRvIII at high levels. GBM14 has non-detectable EGFR WT or EGFRvIII proteins (2, 3). β -actin was used as a loading control.
- B.** Knockdown of DCBLD2 by shRNA (shD2) inhibits EGFRvIII-stimulated Akt activity in primary GBM cells with endogenous EGFRvIII overexpression. Akt and β -actin were used as loading controls.
- C.** Knockdown of DCBLD2 attenuates cell proliferation of GBM6 and GBM39 cells with high levels of endogenous EGFRvIII expression. Cells were seeded in 6 replicates.
- D.** Knockdown of DCBLD2 inhibits soft-agar colony formation of GBM6 and GBM39 cells. Cells were seeded on soft agar in three replicates.
- In panels **C** and **D**, error bars, \pm SD. Compared with shC-treated cells, *, $P < 0.05$. Data are representative of three independent experiments.



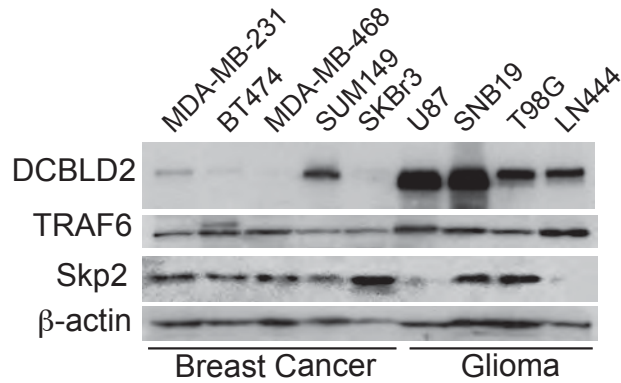
Supplementary Figure 13. EGFRvIII stimulates TRAF6 E3 ligase activity.

IP-IB analyses. HA-TRAF6 and His-Ub were co-expressed with or without EGFRvIII in HEK293T cells. His-Ub was precipitated by Ni-nitrilotriacetic acid (NTA). β -actin was used as a loading control. Data are representative of three independent experiments.



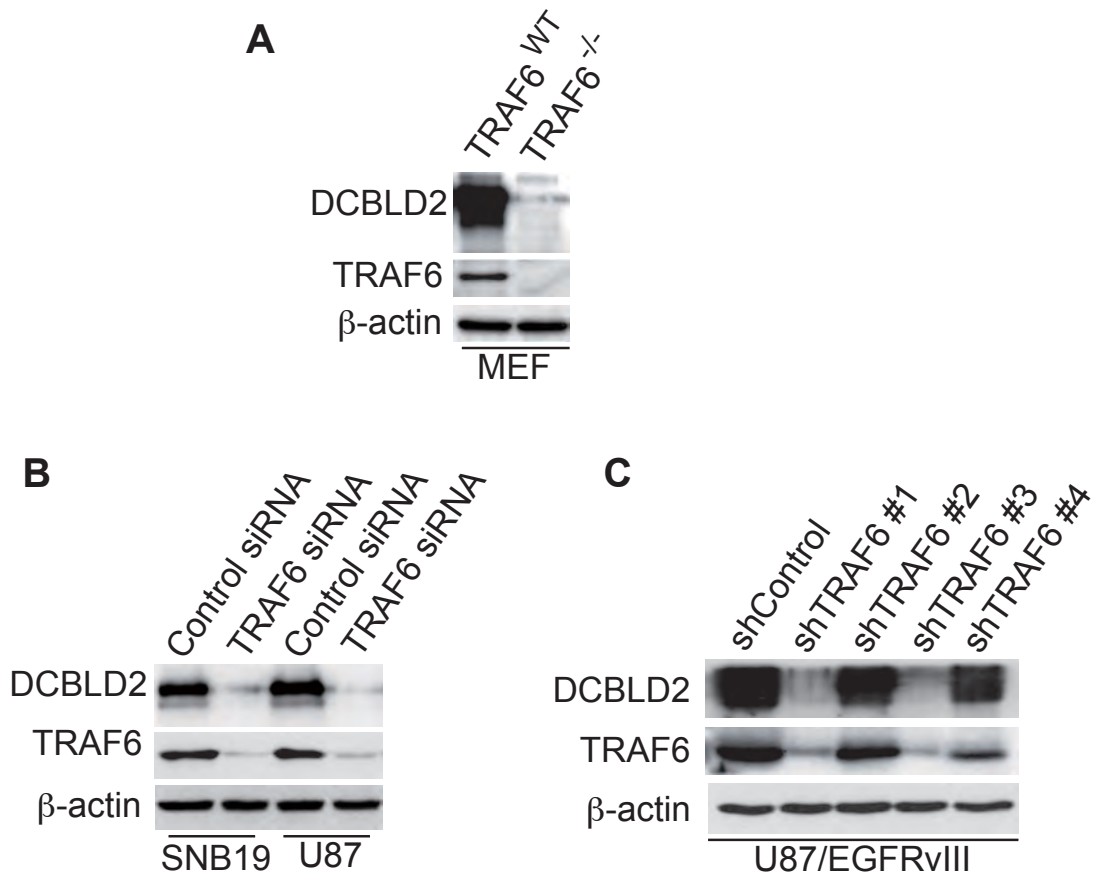
Supplementary Figure 14. Loss of TRAF6 E3 ligase activity has no effect on EGFRvIII-induced association of TRAF6 with DCBLD2.

IP-IB analyses. Flag-DCBLD2 and HA-TRAF6 WT or a C70A mutant was co-expressed with or without EGFRvIII in HEK293T cells. HA-TRAF6, Flag-DCBLD2, and β -actin were used as loading controls. Data are representative of three independent experiments.



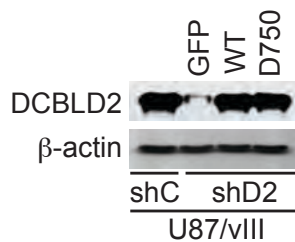
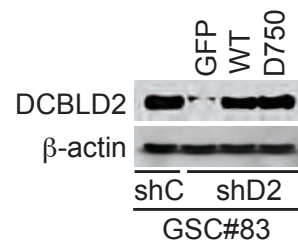
Supplementary Figure 15. Expression of DCBLD2, Skp2, and TRAF6 in human breast cancer and glioma cell lines.

IB analyses. Cell lysates of human cancer cell lines were examined for expression of DCBLD2, TRAF6 and Skp2 with corresponding antibodies. DCBLD2 was detected at low levels in four of five breast cancer cell lines examined. In contrast, DCBLD2 is expressed at high levels in all four glioma cell lines examined here and nine glioma cell lines (including these four) shown in Supplemental Figure 2A. β -actin was used as a loading control. Data are representative of two independent experiments.



Supplementary Figure 16. Inhibition of TRAF6 expression decreases DCBLD2 expression in mouse embryonic fibroblasts (MEF) and glioma cells. IB analyses of expression of DCBLD2 and TRAF6.

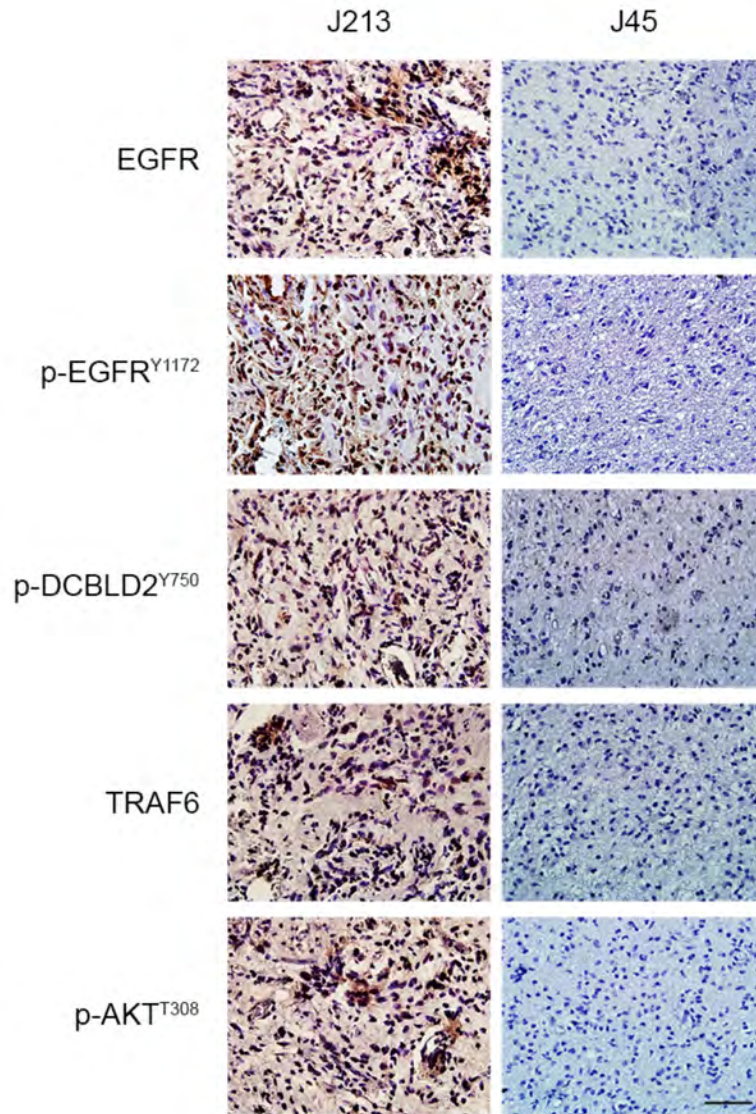
- A.** Expression of endogenous DCBLD2 was at very low levels in TRAF6 null (*TRAF6*^{-/-}) MEF but at high levels in TRAF6 wild type (*TRAF6*^{WT}) MEF.
- B.** Expression of endogenous DCBLD2 was significantly decreased when endogenous TRAF6 was knocked down by siRNAs in glioma SNB19 and U87 cells.
- C.** Expression of endogenous DCBLD2 was markedly decreased when endogenous TRAF6 was knocked down by two separate shRNAs, #1 and #3, but not shRNAs #2 and #4, or a control shRNA in glioma U87/EGFRvIII cells. β-actin was used as a loading control. Data are representative of two independent experiments.

A**B**

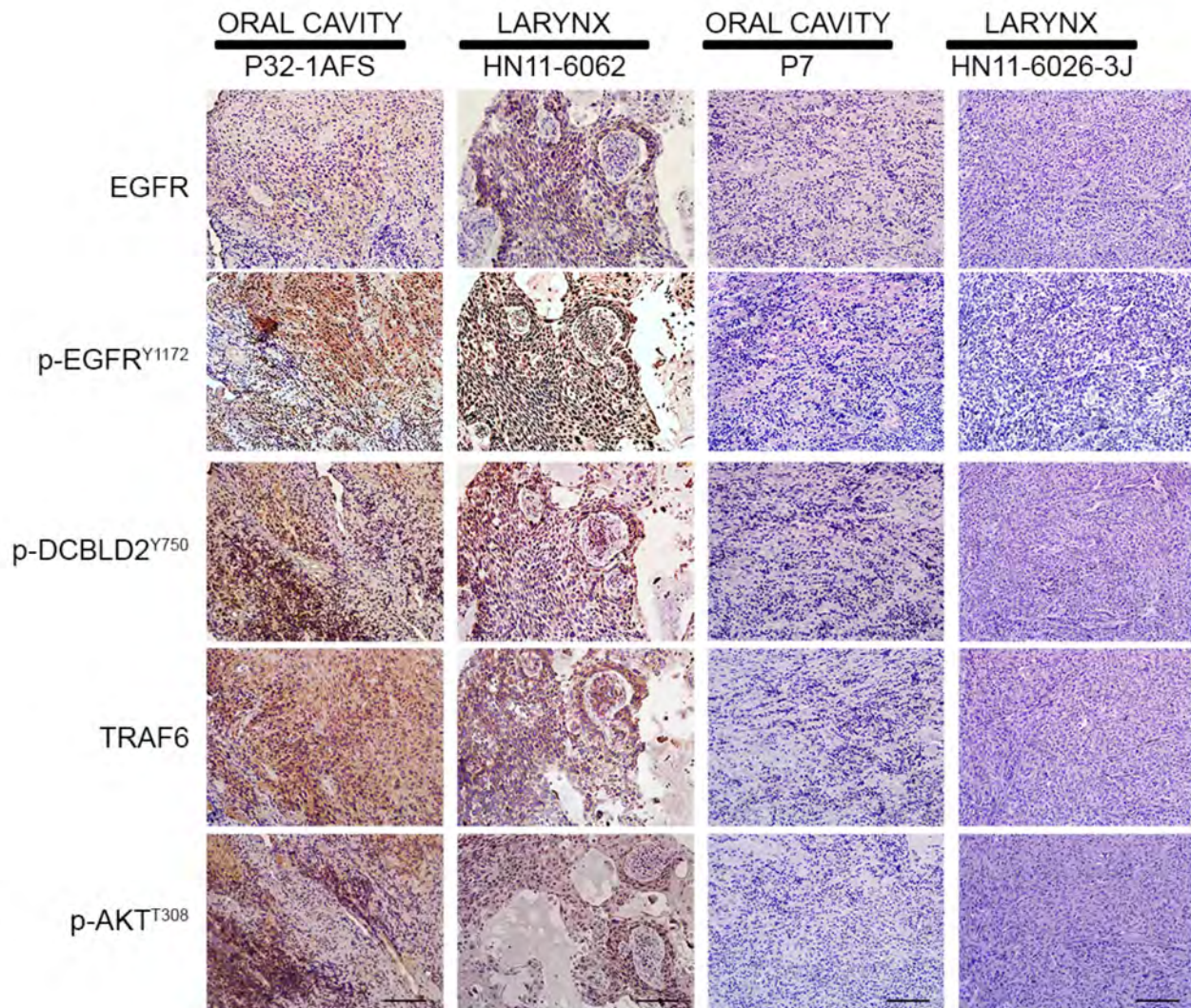
Supplementary Figure 17. Re-expression of DCBLD2 WT or DY750 mutant in glioma U87 cells or patient-derived glioma stem cells (GSC#83) that endogenous DCBLD2 was knocked down by shRNA for DCBLD2 (shD2).

IB analyses. Cell lysates of various U87 or patient-derived glioma stem cells (GSC#83) (4) were examined for expression of DCBLD2^{WT} or DCBLD2^{D750} mutant. shC, cells expressed a scrambled control shRNA. shD2, cells expressed a shRNA for DCBLD2. GFP, cells expressed GFP, WT, cells express DCBLD2^{WT} and D750, cells expressed DCBLD2^{D750} mutant. β -actin was used as a loading control. Data are representative of two independent experiments.

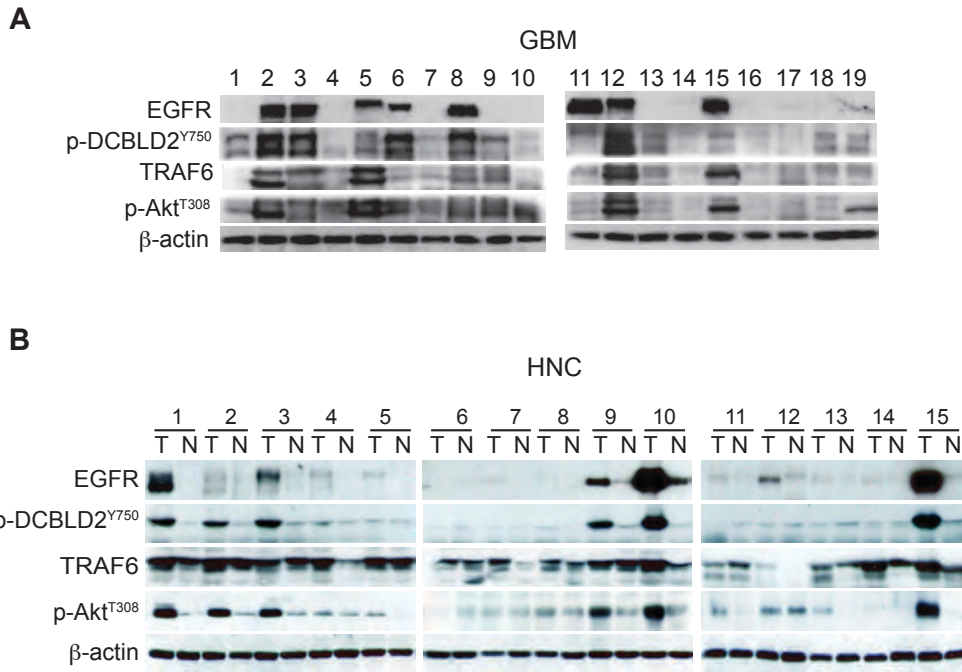
+



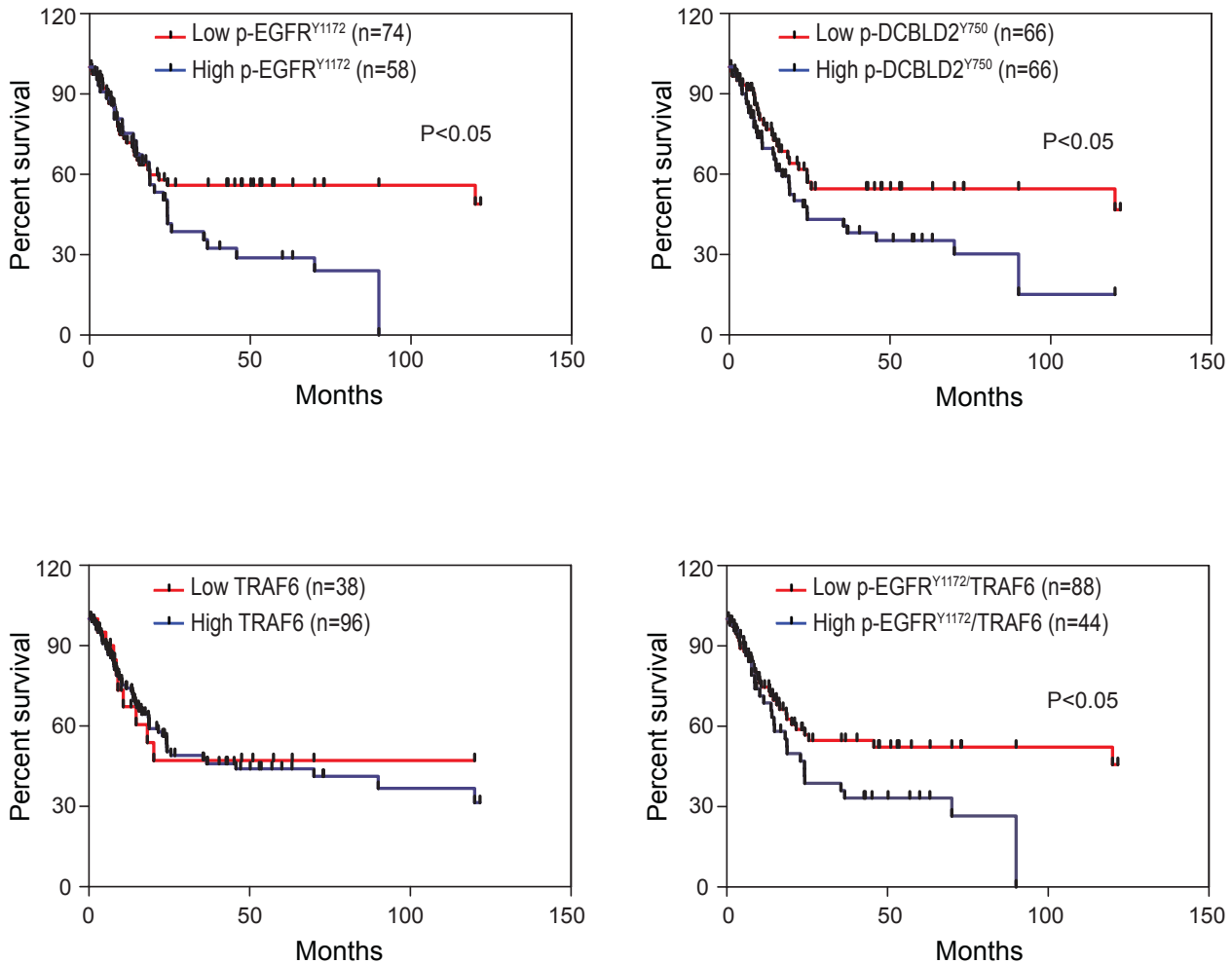
Supplementary Figure 18. Examples of a clinical GBM sample showing co-expression of EGFR, p-EGFR^{Y1172}, p-DCBLD2^{Y750}, TRAF6, and p-Akt^{T308} and a GBM sample with negative staining for these proteins. Representative images of two GBM specimens that were IHC stained positive (J213) or negative (J45) by indicated antibodies. Scale bars, 50 μ m. IHC analyses on these two GBM samples using these five antibodies were performed twice. Data are representative of two independent experiments.



Supplementary Figure 19. Examples of two clinical HNC samples showing co-expression of EGFR, p-EGFR^{Y1172}, p-DCBLD2^{Y750}, TRAF6, and p-Akt^{T308} and two HNC samples with negative staining for these proteins. Representative images of two HNC specimens that were IHC stained positive (P32-1AFS and HN11-6062) and two HNC tissues that showed negative staining (P7 and HN11-6026-3J) by indicated antibodies. Scale bars, 100 μ m. IHC analyses on these HNC samples in TMAs using these five antibodies were performed twice. Data are representative of two independent experiments.

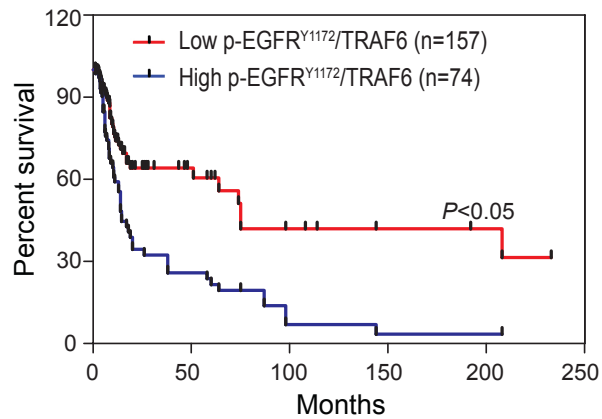
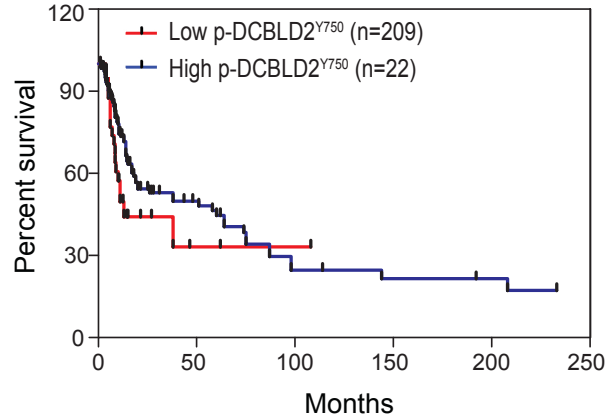
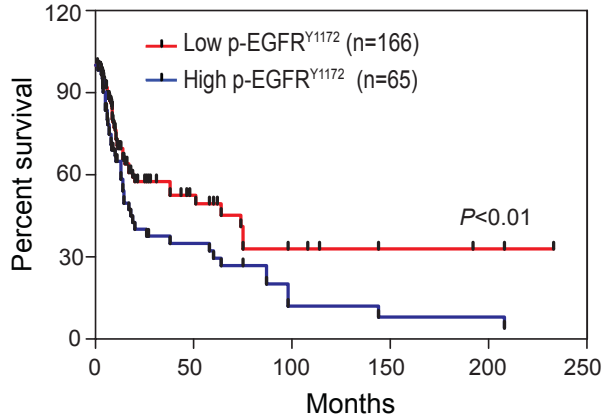


Supplementary Figure 20. Expression of EGFR, p-DCBLD2^{Y750}, TRAF6 and p-Akt in separate cohorts of 19 GBM specimens, 15 HNC samples and their matched normal tissues. IB analyses of expression of EGFR, p-DCBLD2^{Y750}, TRAF6 and p-Akt^{T308} in 19 snap-frozen clinical GBM specimens (A), 15 snap-frozen HNC samples (T) and their matched normal tissues (N) (B). β-actin was used as a loading control. Data are representative of 2 independent experiments.



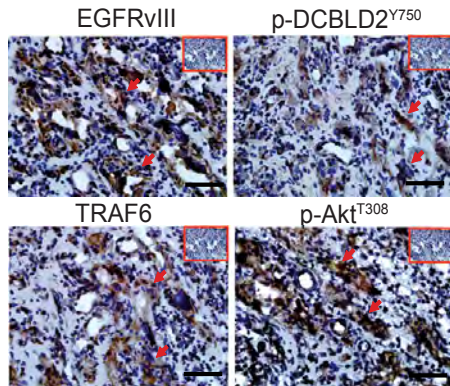
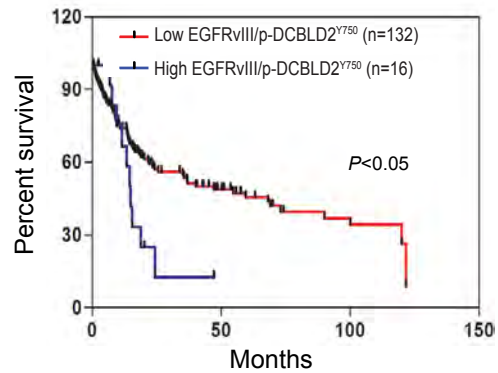
Supplementary Figure 21. High expression of either p-EGFR^{Y1172} or p-DCBLD2^{Y750}, or co-expression of p-EGFR^{Y1172} with TRAF6, correlates with worse survival of patients with gliomas.

Kaplan-Meier analyses of patients with high p-EGFR^{Y1172}, p-DCBLD2^{Y750}-expressing, or co-expression of p-EGFR^{Y1172}-TRAF6 tumors (blue line) versus low p-EGFR^{Y1172}, p-DCBLD2^{Y750}-expressing or low co-expression of p-EGFR^{Y1172}-TRAF6 tumors (red line) in IHC-stained WHO grades II-IV glioma specimens showed in Figure 8A and Supplemental Table 1. Expression of TRAF6 does not correlate with clinical outcomes. *P* values were calculated by using log-rank test. Black bars, censored data.



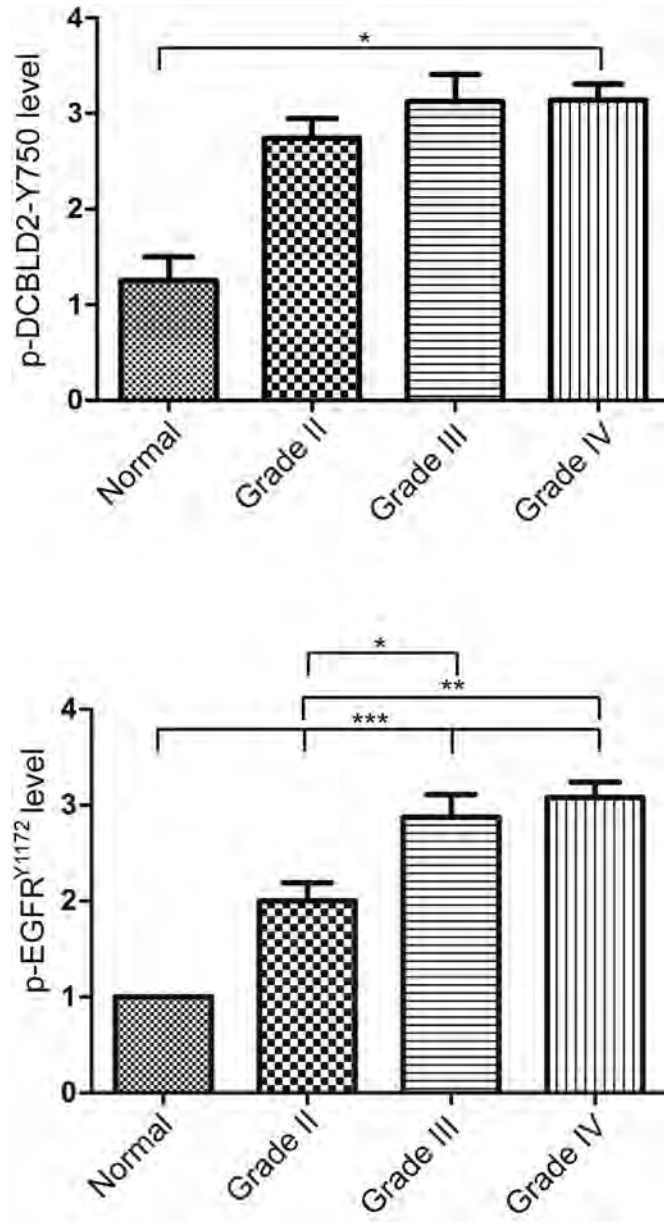
Supplementary Figure 22. High expression of p-EGFR^{Y1172} or co-expression of EGFR with TRAF6 correlates with worse survival of patients with HNCs.

Kaplan-Meier analyses of patients with high expression of p-EGFR^{Y1172}, p-DCBLD2^{Y750} or co-expression of p-EGFR^{Y1172}-TRAF6 tumors (blue line) versus low p-EGFR^{Y1172} p-DCBLD2^{Y750} or p-EGFR^{Y1172}-TRAF6-expressing tumors (red line) in IHC-stained TMA of HNCs showed in Figure 8C and Supplemental Table 2. Expression of p-DCBLD2^{Y750} does not correlate with clinical outcomes. *P* values were calculated by using log-rank test. Black bars, censored data.

A**B**

Supplementary Figure 23. EGFRvIII, p-DCBLD2^{Y750}, TRAF6, and p-Akt^{T308} are co-expressed in clinical gliomas and co-expression of EGFRvIII with p-DCBLD2^{Y750} correlates with poor survival of patients with gliomas

- A.** A total of 148 clinical primary glioma specimens including WHO grade I to IV tumors were analyzed by IHC for p-DCBLD2^{Y750}, TRAF6, p-Akt^{T308} and EGFRvIII. Representative images of serial sections of a grade IV GBM tissue using anti-EGFRvIII (clone 8.3), anti-p-DCBLD2^{Y750}, anti-TRAF6, and anti-p-Akt^{T308} antibodies are shown. Inserts, isotype-matched IgG controls of the same area in adjacent sections. Arrows, positive staining. Scale bars, 50 μ m. IHC analyses on these glioma tumor samples using these four antibodies were performed twice. Data are representative of two independent experiments.
- B.** Kaplan-Meier analyses of patients with high EGFRvIII/p-DCBLD2^{Y750}-expressing tumors (blue line) versus low EGFRvIII/p-DCBLD2^{Y750}-expressing tumors (red line) in IHC staining assays (A) of WHO grades I-IV gliomas. *P* values were calculated by using log-rank test. Black bars, censored data.



Supplementary Figure 24. The levels of expression of p-DCBLD2^{Y750} and p-EGFR^{Y1172} are increased in WHO tumor grade II to IV clinical gliomas compared with normal brain tissues.

IHC staining of 31 WHO grade II, 23 grade III and 78 grade IV (GBM) glioma specimens using anti-EGFR^{Y1172} or anti-p-DCBLD2^{Y750} antibodies with validated specificities. The data were compared with four IHC-stained normal brains that had no detectable pathological lesions. *, $P < 0.05$, **, $P < 0.01$ and ***, $P < 0.001$.

Supplementary Table 1. Spearman's rank correlation analysis of expression level of p-EGFR^{Y1172}, p-DCBLD2^{Y750}, TRAF6 and p-Akt^{T308} in human clinical glioma specimens by IHC staining.

r	p-EGFR ^{Y1172}	p-DCBLD2 ^{Y750}	TRAF6	p-AKT ^{T308}
p-EGFR ^{Y1172}	1.0 ^c	0.5 ^c	0.4 ^c	0.2 ^a
p-DCBLD2 ^{Y750}	0.5 ^c	1.0 ^c	0.2 ^b	0.3 ^c
TRAF6	0.4 ^c	0.2 ^b	1.0 ^c	0.5 ^c
p-AKT ^{T308}	0.2 ^a	0.3 ^c	0.5 ^c	1.0 ^c

Note: a. $P < 0.05$; b. $P < 0.01$ and c. $P < 0.001$

Supplementary Table 2. Spearman's rank correlation analysis of expression level of p-EGFR^{Y1172}, p-DCBLD2^{Y750}, TRAF6 and p-Akt^{T308} in human clinical HNC specimens by IHC staining.

r	p-EGFR ^{Y1172}	p-DCBLD2 ^{Y750}	TRAF6	p-Akt ^{T308}
p-EGFR ^{Y1172}	1.0 ^c	0.2 ^a	0.4 ^c	0.1
p-DCBLD2 ^{Y750}	0.2 ^a	1.0 ^c	0.2 ^b	0.3 ^c
TRAF6	0.4 ^c	0.2 ^b	1.0 ^c	0.1
p-AKT ^{T308}	0.1	0.3 ^b	0.1	1.0 ^c

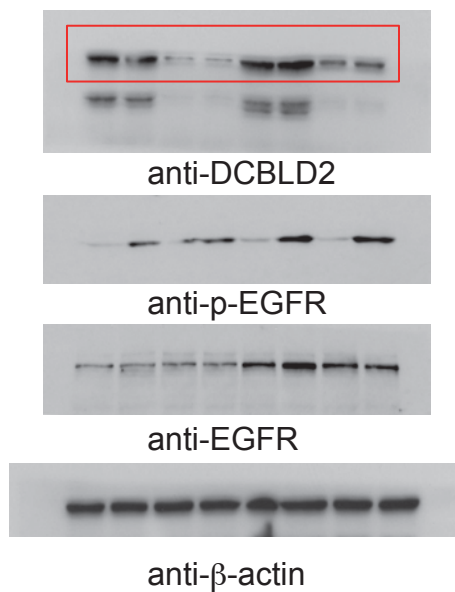
Note: a. $P < 0.05$; b. $P < 0.01$ and c. $P < 0.001$

References:

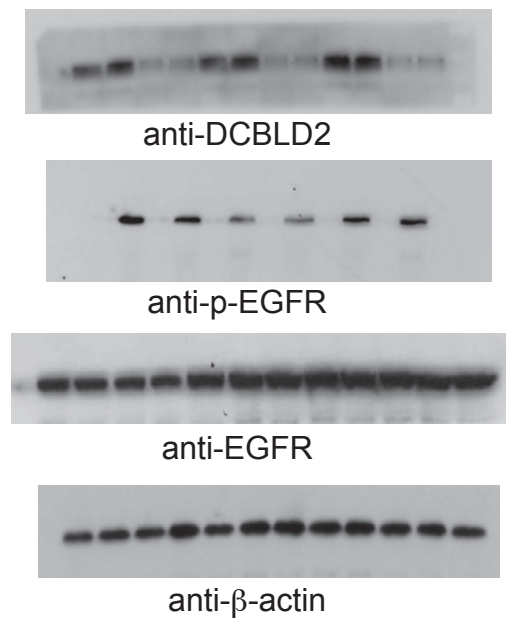
1. Inda, M.M., et al. Tumor heterogeneity is an active process maintained by a mutant EGFR-induced cytokine circuit in glioblastoma. *Genes Dev* 2010; 24(16):1731-1745.
2. Giannini, C., et al. Patient tumor EGFR and PDGFRA gene amplifications retained in an invasive intracranial xenograft model of glioblastoma multiforme. *Neuro-oncol* 2005; 7(2):164-176.
3. Yiin, J.J., et al. ZD6474, a multitargeted inhibitor for receptor tyrosine kinases, suppresses growth of gliomas expressing an epidermal growth factor receptor mutant, EGFRvIII, in the brain. *Mol Cancer Ther* 2010; 9(4):929-941.
4. Mao, P., et al. Mesenchymal glioma stem cells are maintained by activated glycolytic metabolism involving aldehyde dehydrogenase 1A3. *Proc Natl Acad Sci U S A* 2013; 110(21):8644-8649.

Full unedited gels for Figure 1

A

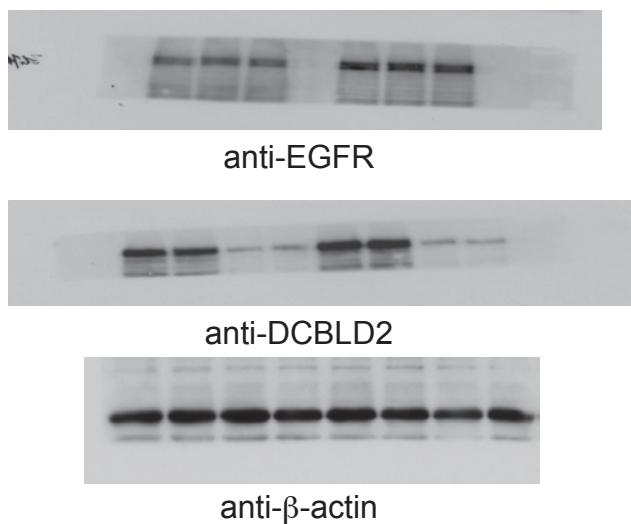


D

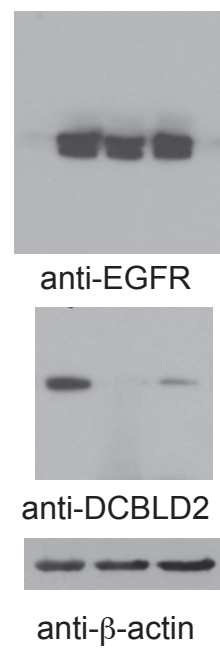


Full unedited gels for Figure 2

A

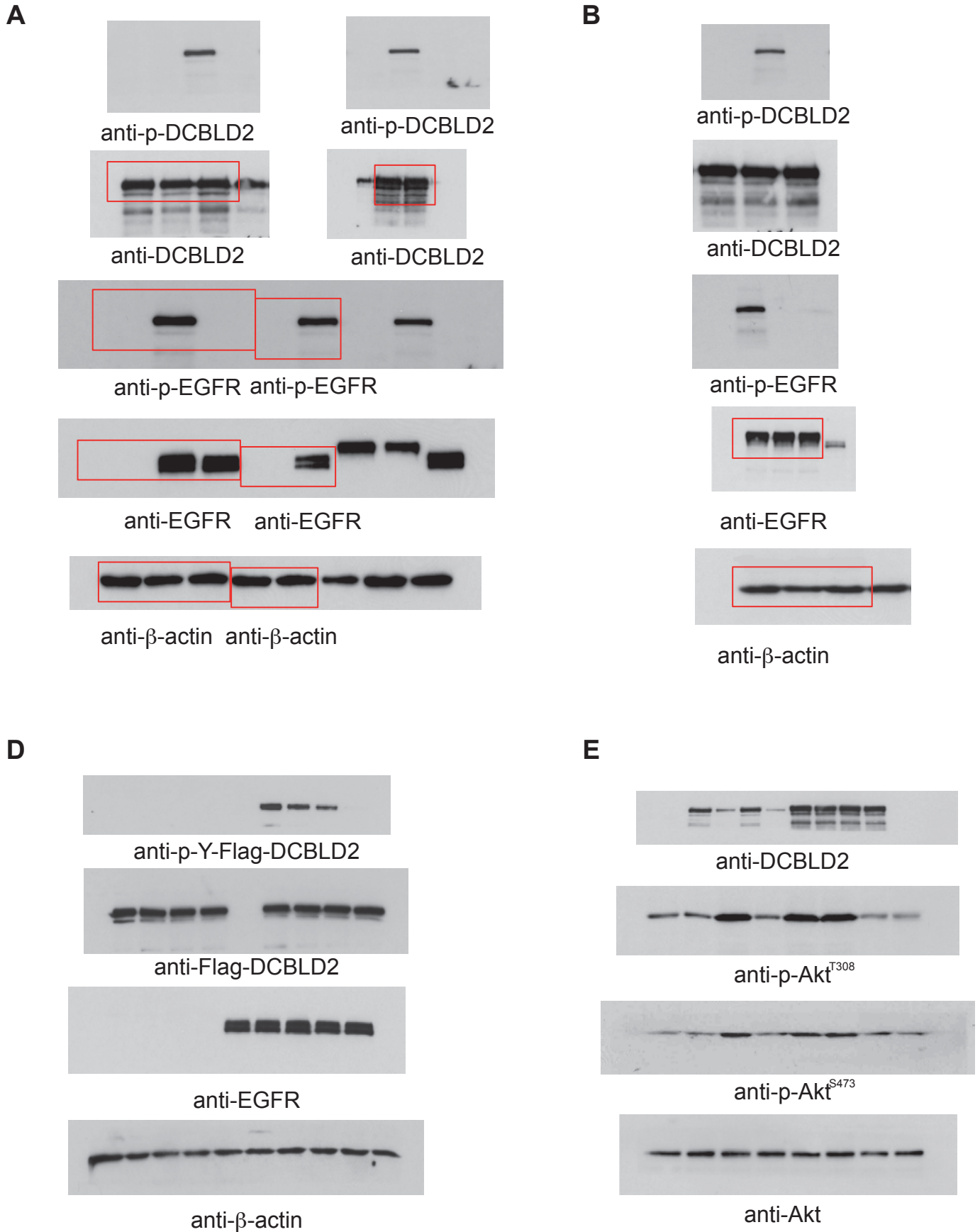


G



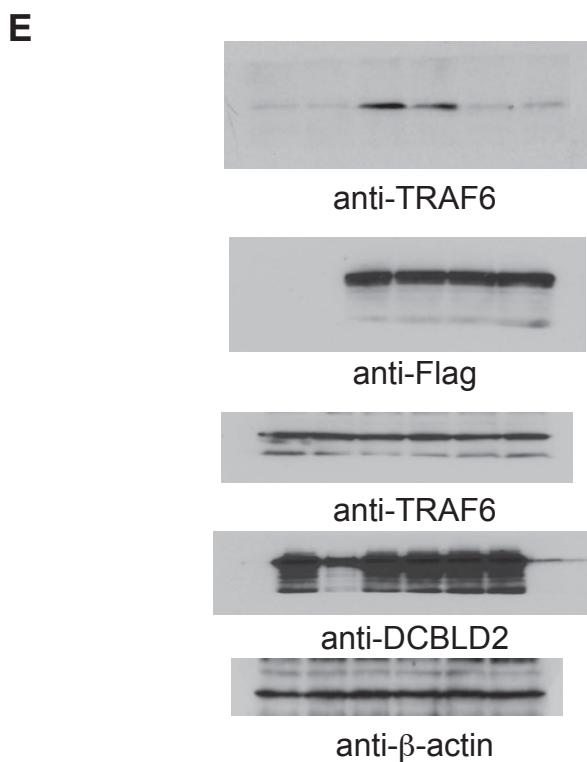
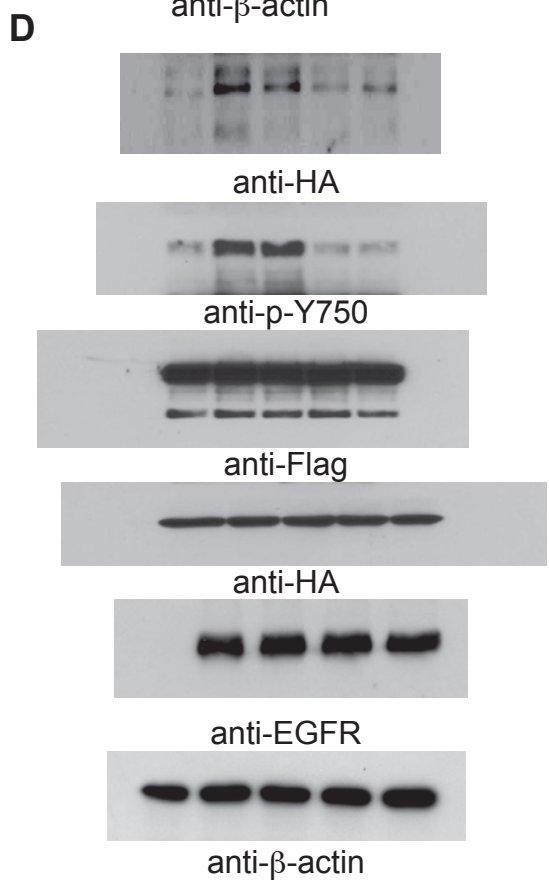
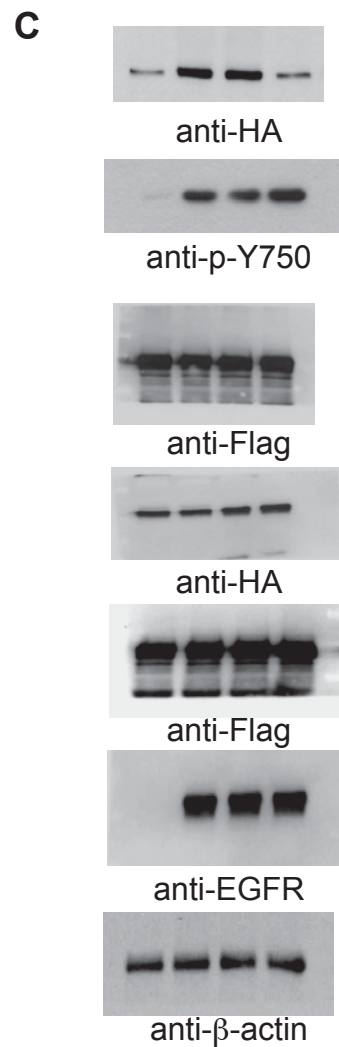
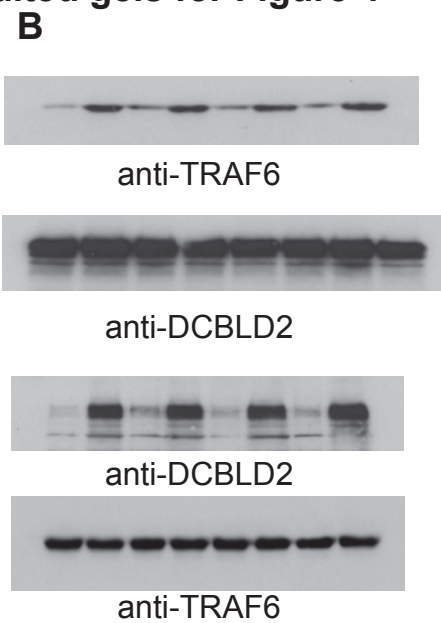
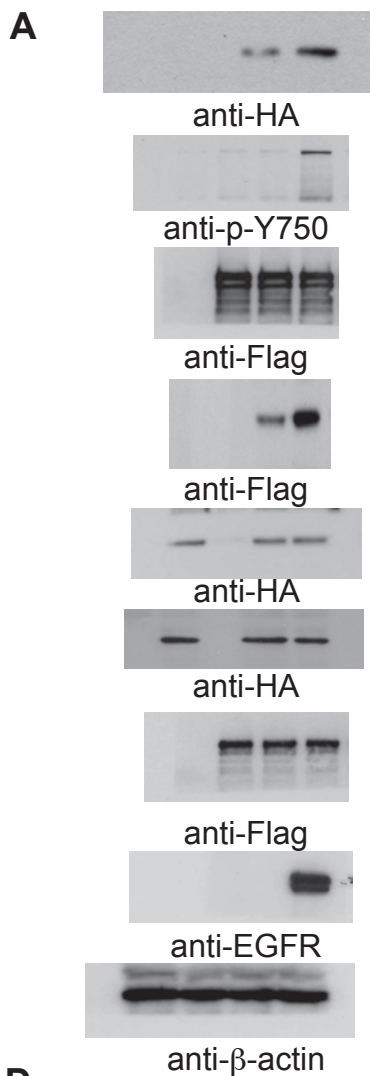
Rectangles indicate cropped areas used in indicated Figures

Full unedited gels for Figure 3



Rectangles indicate cropped areas used in indicated Figures

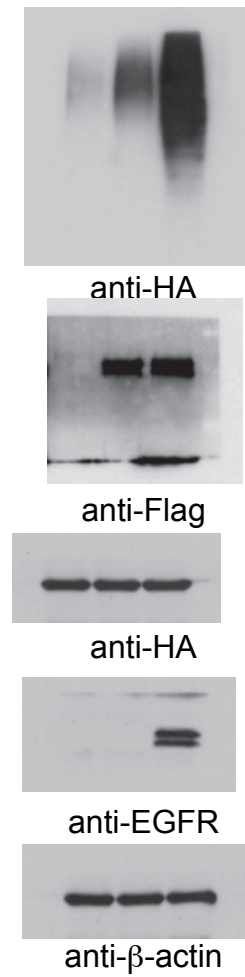
Full unedited gels for Figure 4



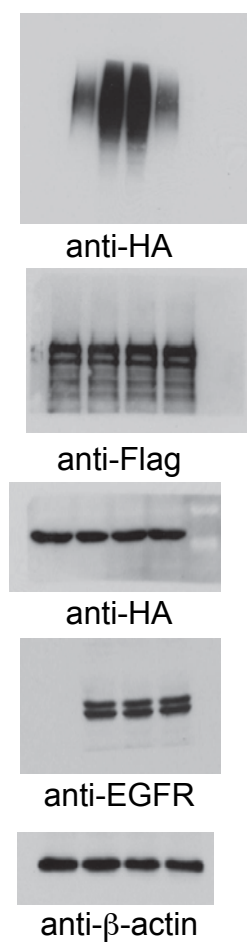
Rectangles indicate cropped areas used in indicated Figures

Full unedited gels for Figure 5

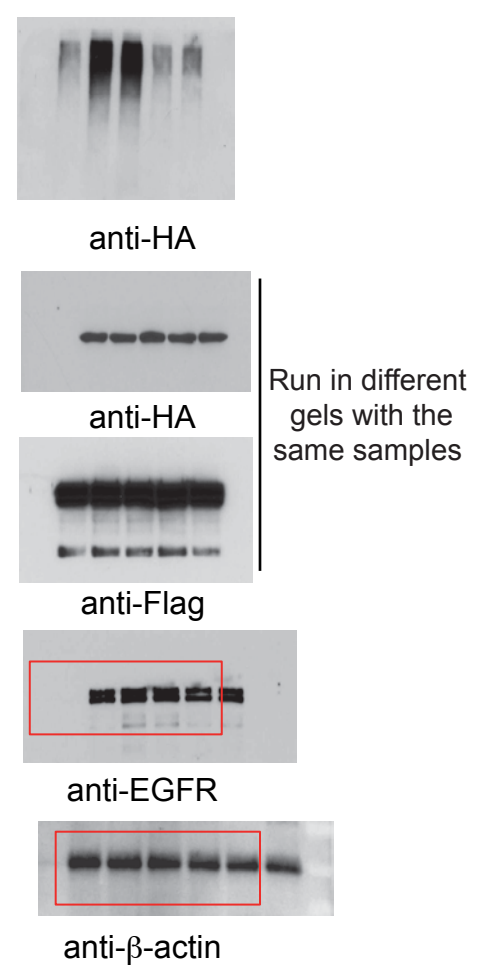
A



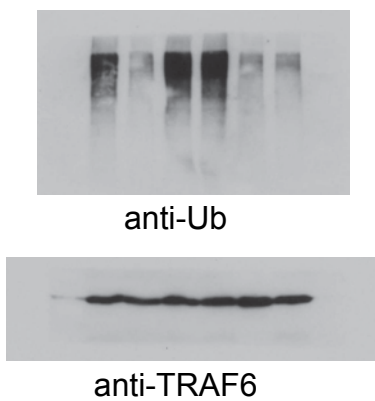
B



C



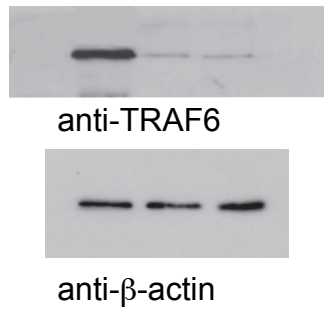
D



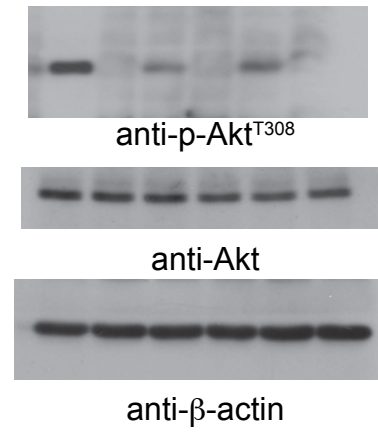
Rectangles indicate cropped areas used in indicated Figures

Full unedited gels for Figure 6

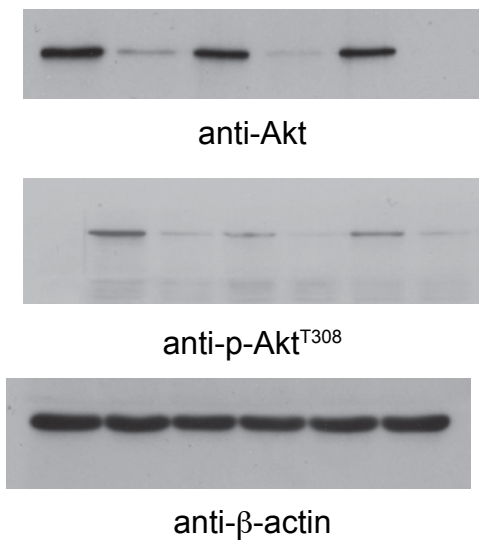
A



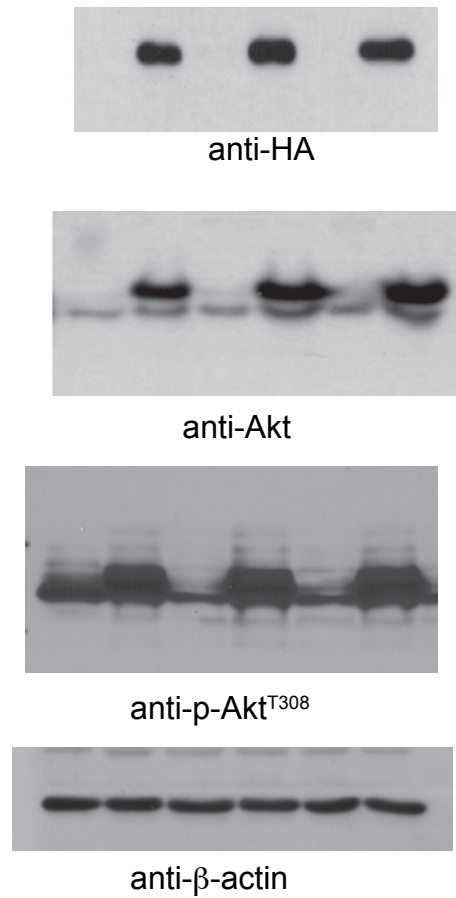
C



D

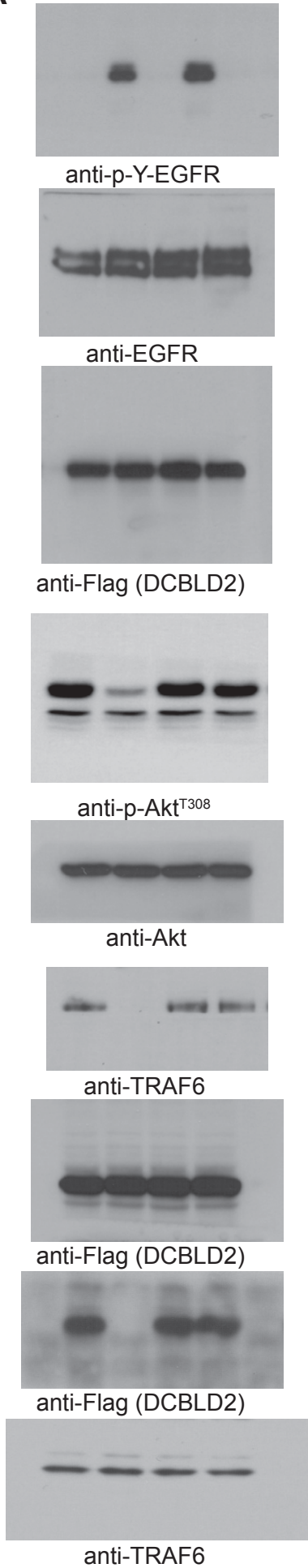


E



Full unedited gels for Figure 7

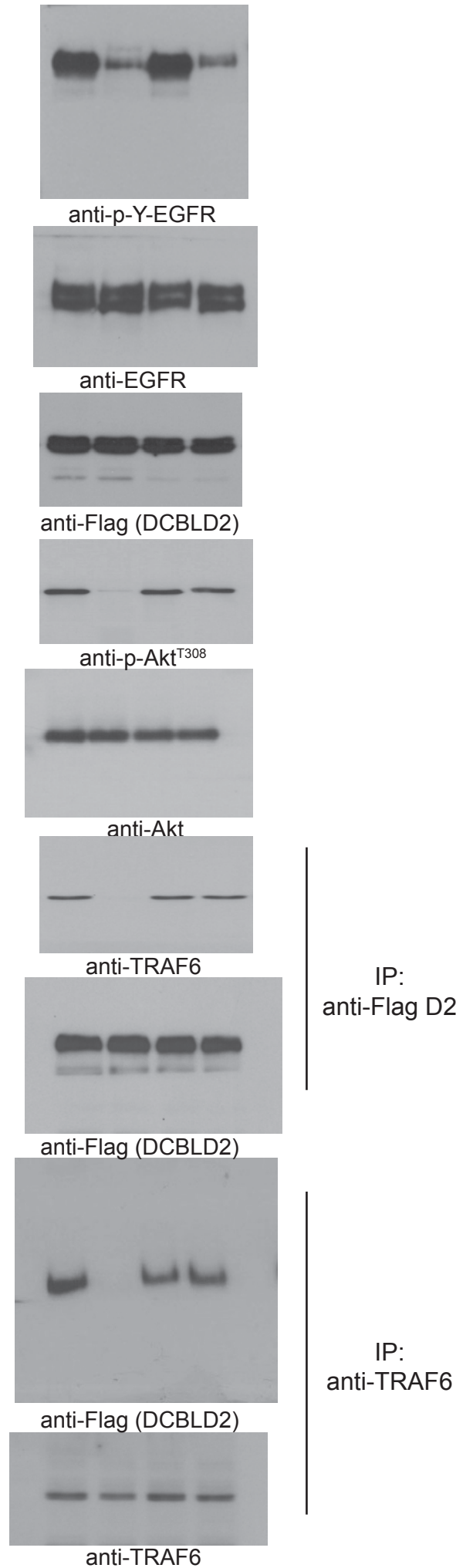
A



IP:
anti-Flag D2

IP:
anti-TRAF6

C

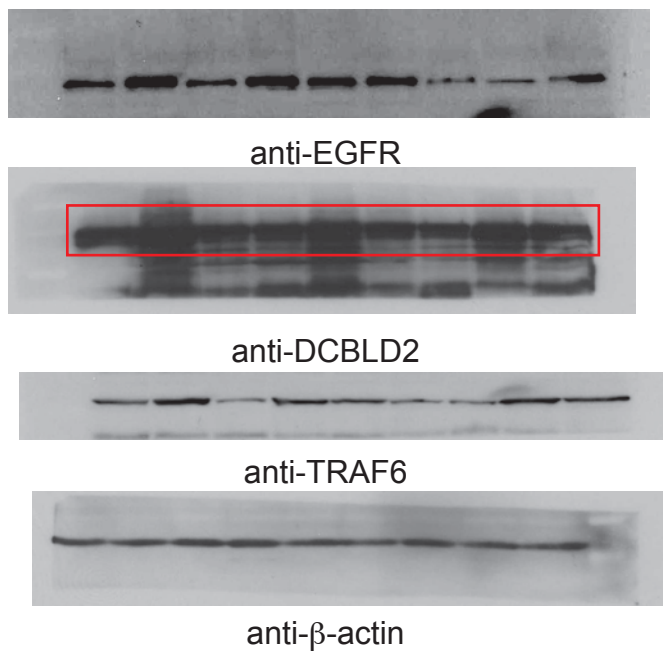


IP:
anti-Flag D2

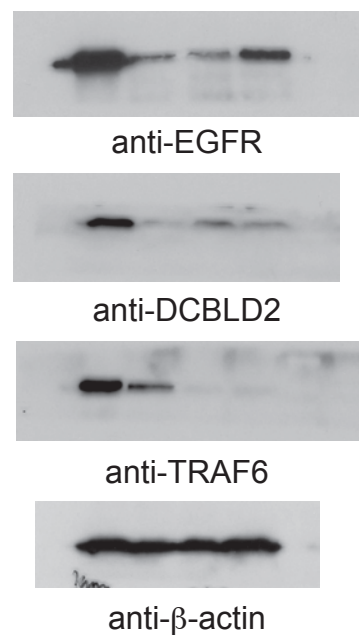
IP:
anti-TRAF6

Full unedited gels for Supplemental Figure 2

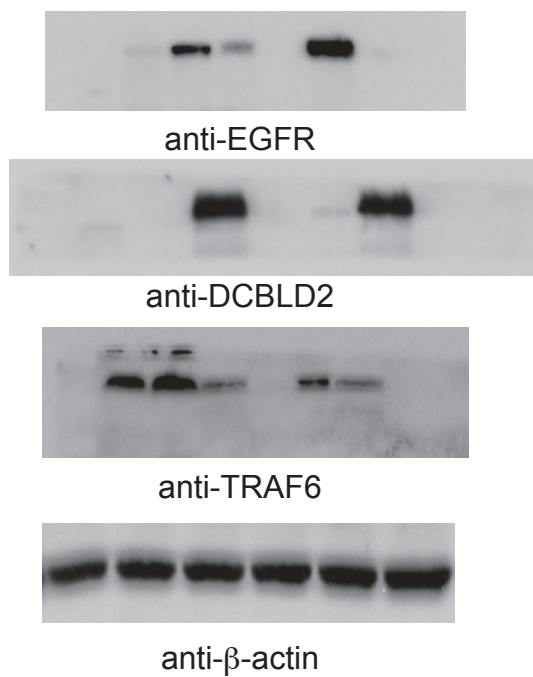
A



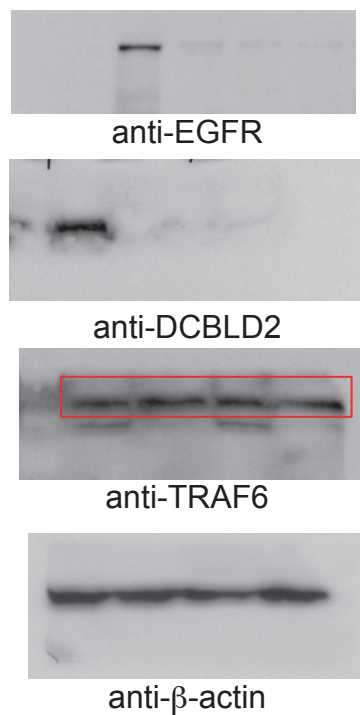
B



C



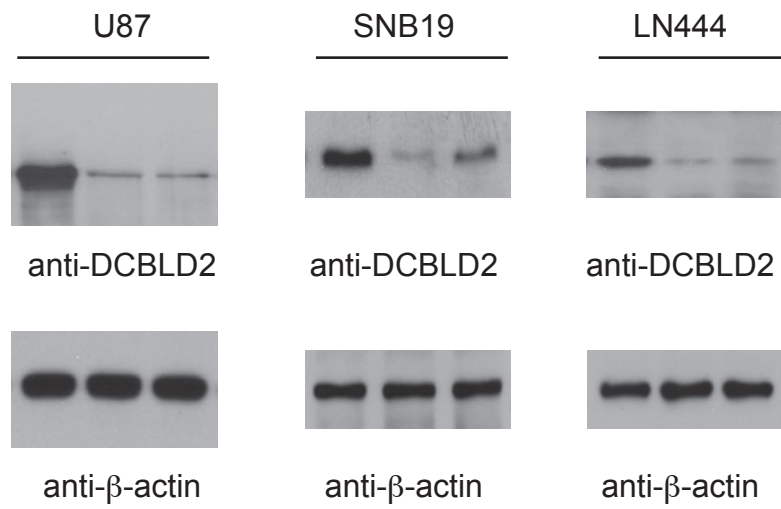
D



Rectangles indicate cropped areas used in indicated Figures

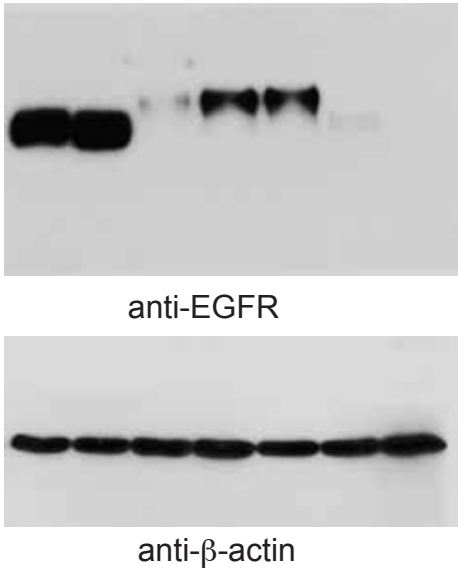
Full unedited gels for Supplemental Figure 3

A

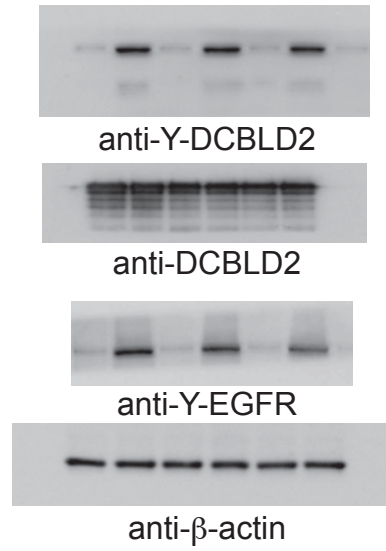


Full unedited gels for the indicated Figures

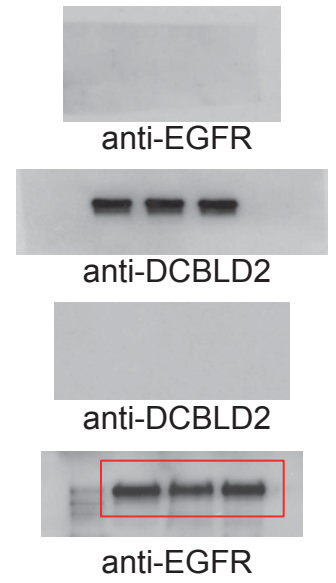
Supplemental Figure 4C



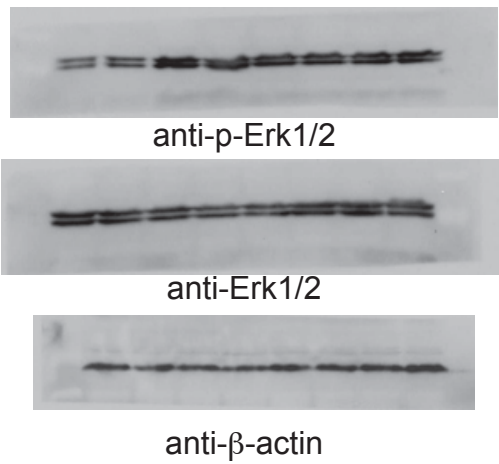
Supplemental Figure 5



Supplemental Figure 6

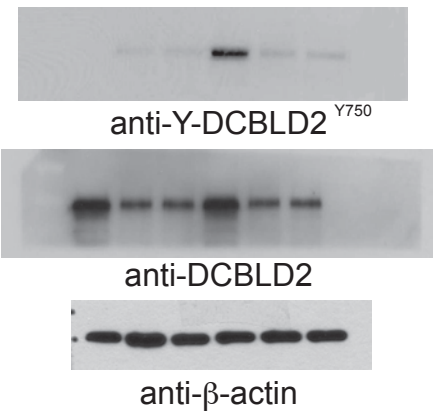


Supplemental Figure 7

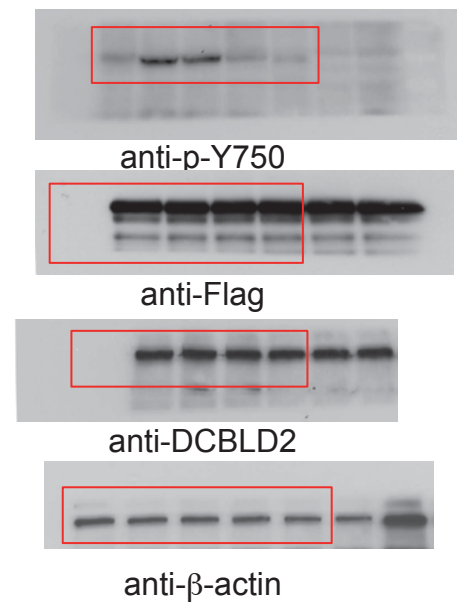


Supplemental Figure 9

A



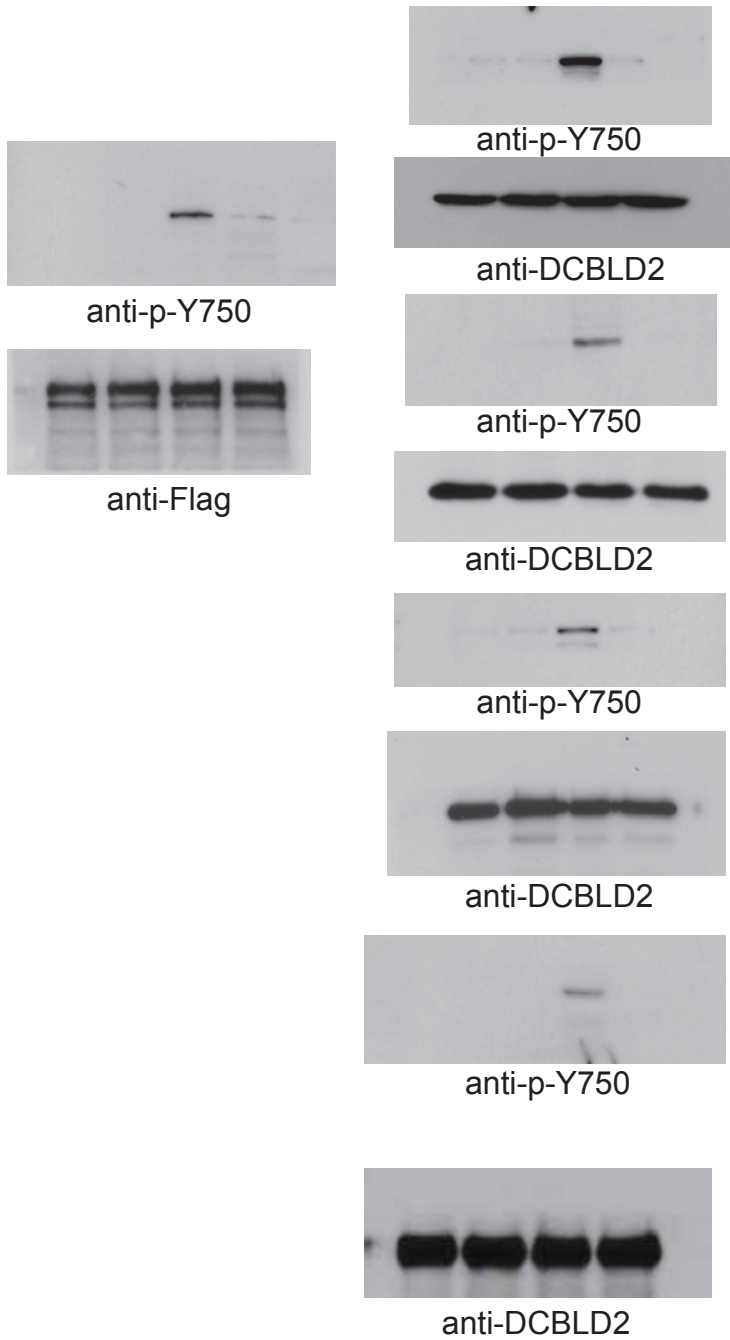
B



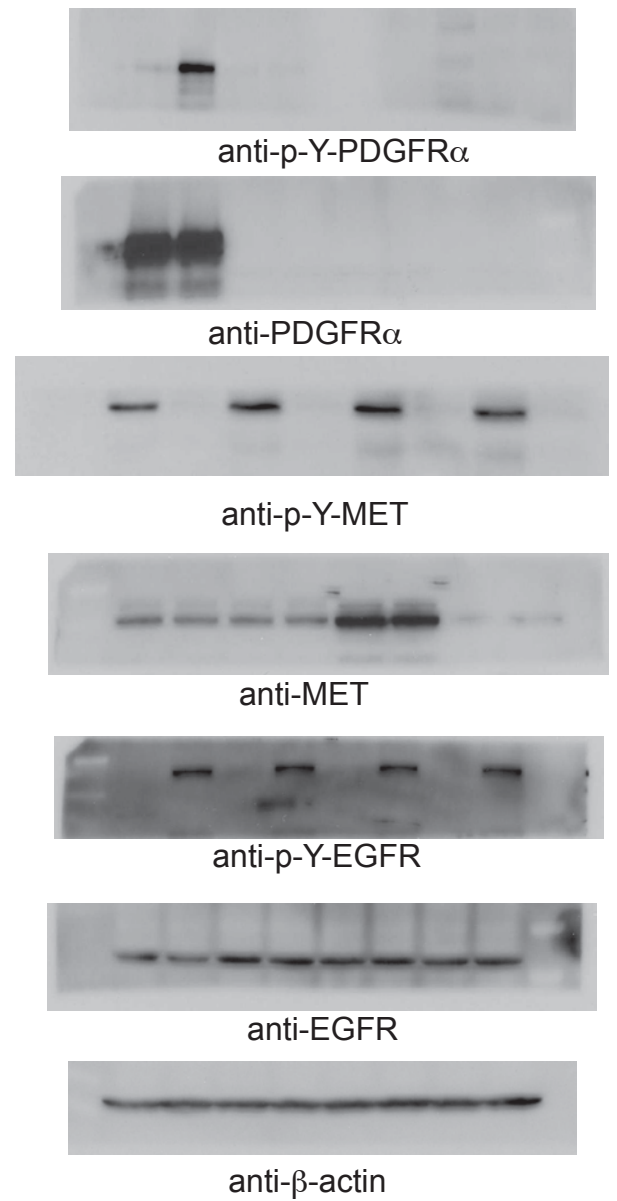
Rectangles indicate cropped areas used in indicated Figures

Full unedited gels for the indicated Figures

Supplemental Figure 10



Supplemental Figure 11



Rectangles indicate cropped areas used in indicated Figures

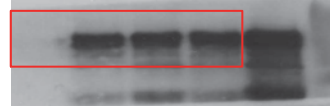
Full unedited gels for the indicated Figures

Supplemental Figure 12

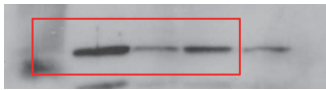
A



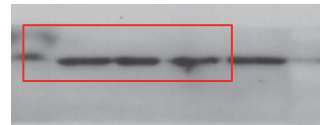
anti-EGFR



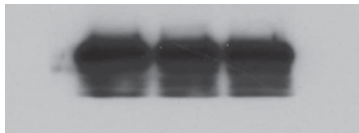
anti-DCBLD2



anti-TRAF6



anti- β -actin



anti-DCBLD2

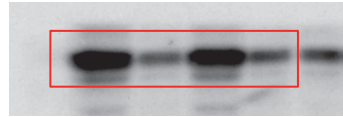


anti-Y-DCBLD2^{Y750}

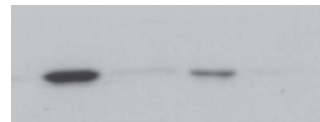


anti-TRAF6

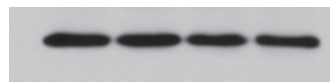
B



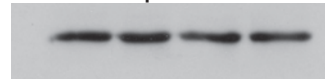
anti-DCBLD2



anti-p-Akt^{T308}



anti-p-Akt

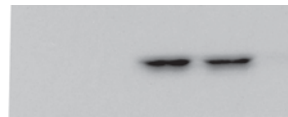


anti- β -actin

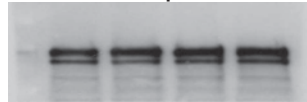
Supplemental Figure 14



anti-HA



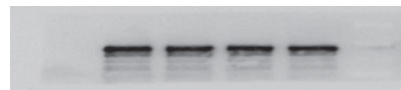
anti-p-Y750



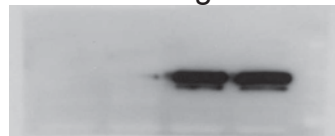
anti-Flag



anti-HA



anti-Flag



anti-EGFR

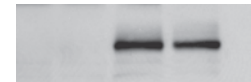


anti- β -actin

Supplemental Figure 13



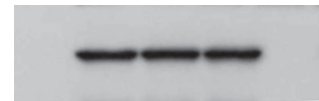
anti-HA



anti-HA

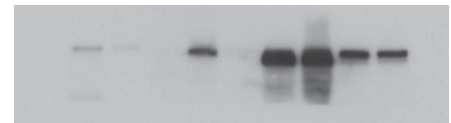


anti-EGFR



anti- β -actin

Supplemental Figure 15



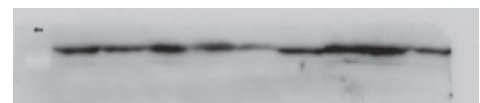
anti-DCBLD2



anti-TRAF6



anti-Spk2

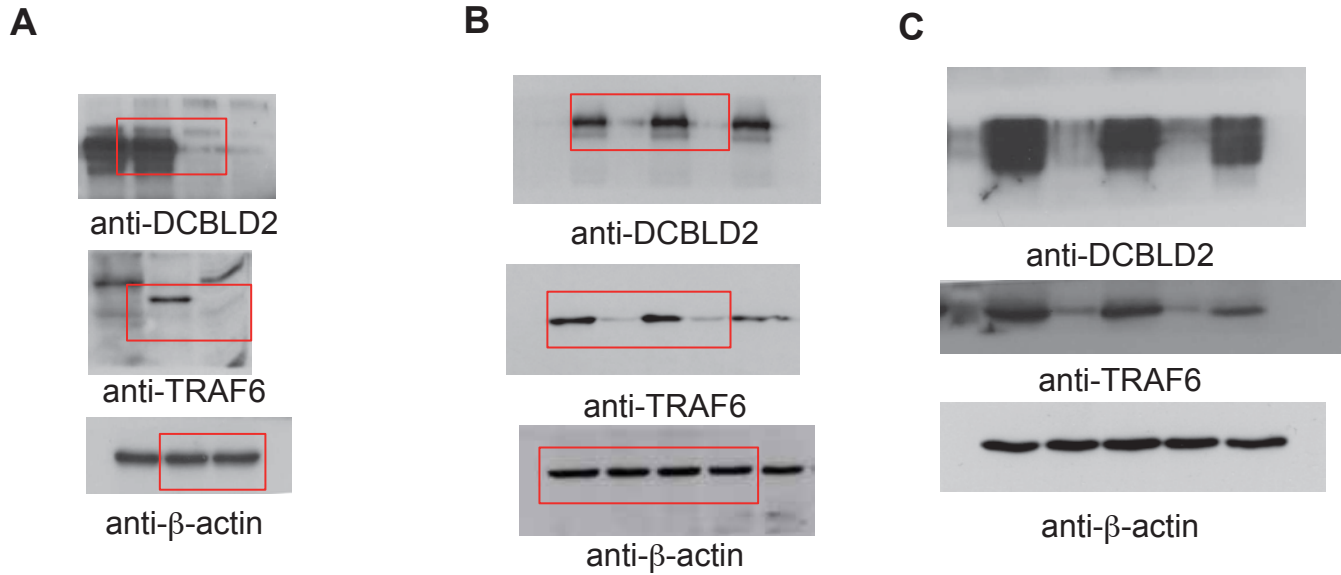


anti- β -actin

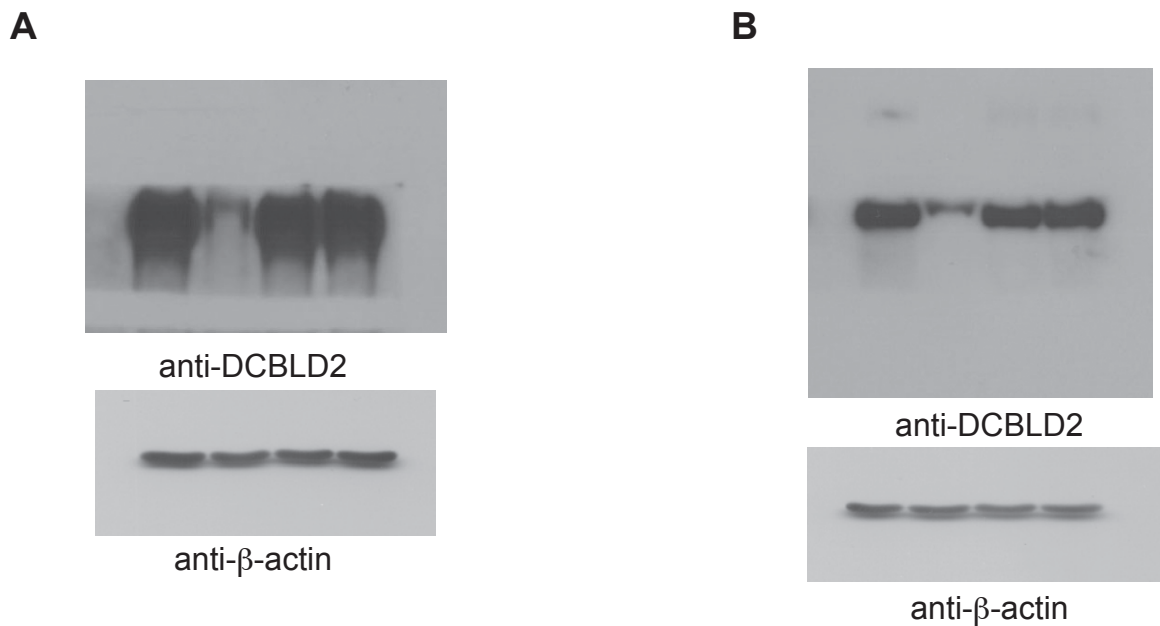
Rectangles indicate cropped areas used in indicated Figures

Full unedited gels for the indicated Figures

Supplemental Figure 16



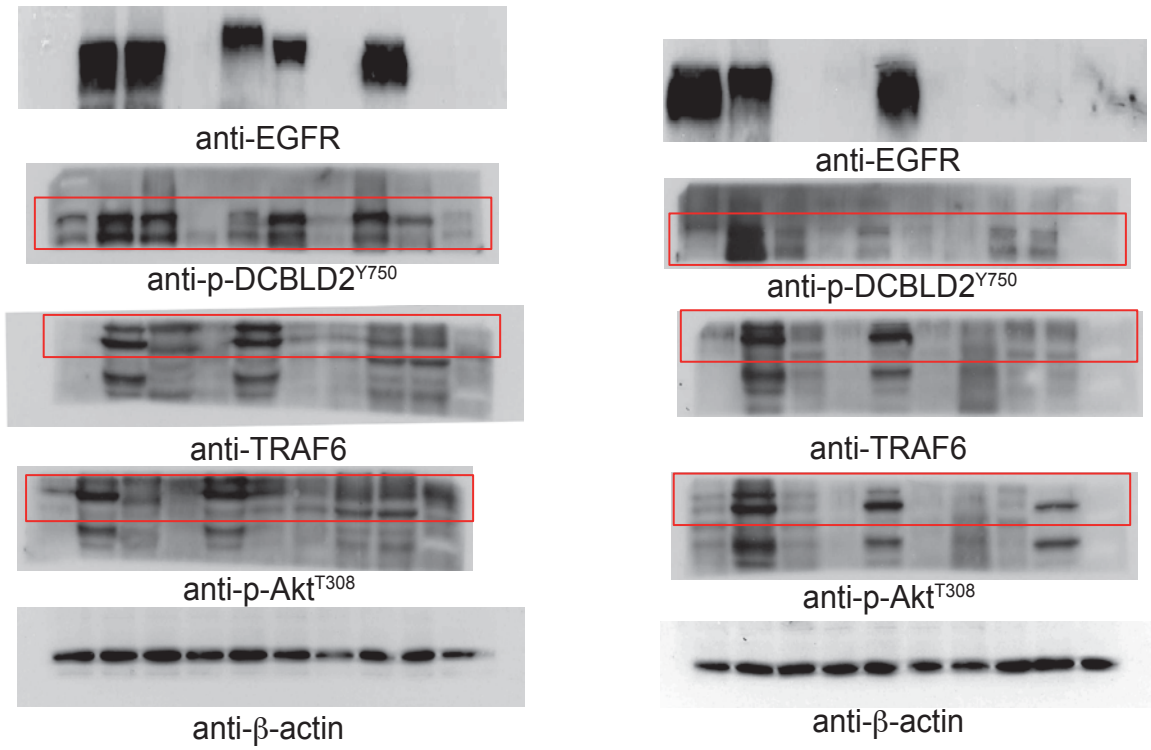
Supplemental Figure 17



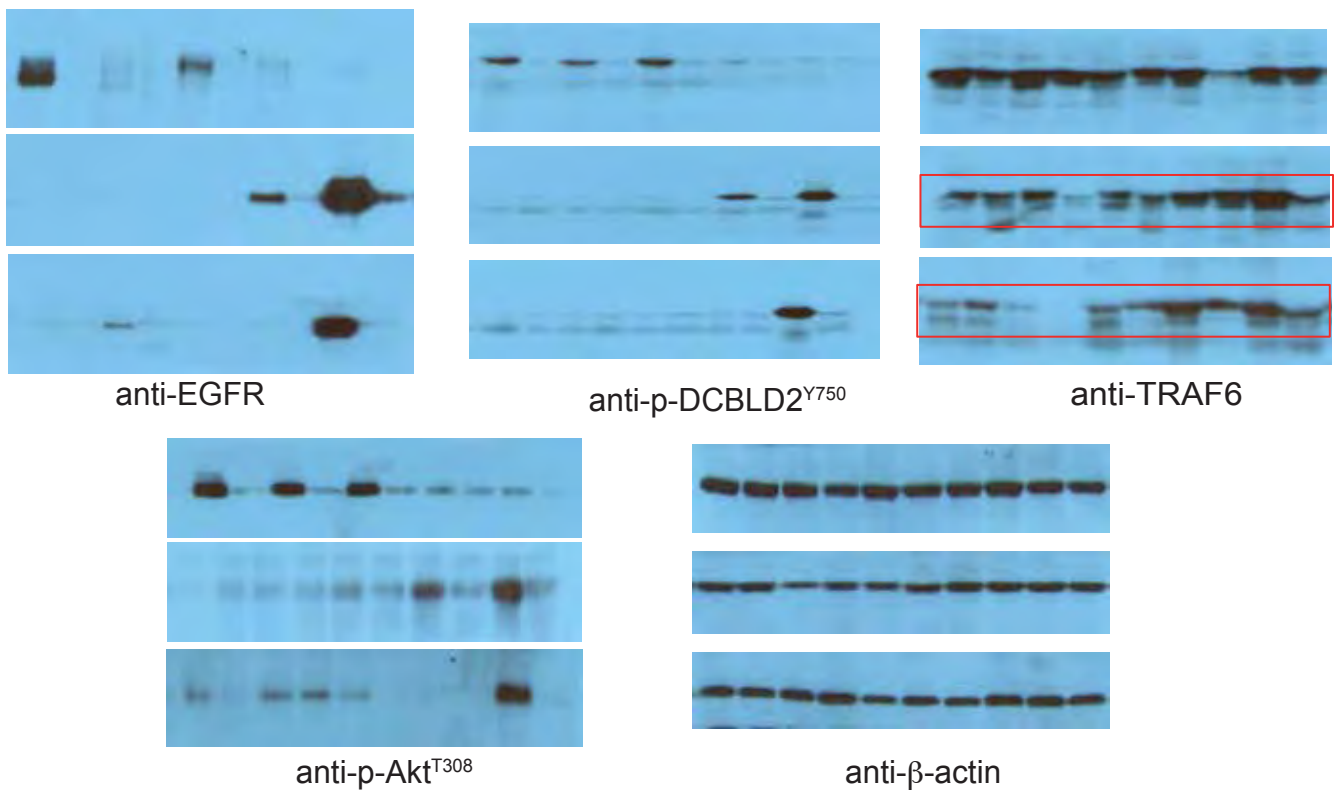
Rectangles indicate cropped areas used in indicated Figures

Full unedited gels for Supplemental Figure 20

A



B



Rectangles indicate cropped areas used in the indicated Figures.